

HUMAN PILOT DYNAMICS WITH VARIOUS MANIPULATORS

D. T. McRuer
R. E. Magdaleno

The distribution of this document is unlimited.

FOREWORD

This report documents an analytical and experimental investigation of human pilot dynamics accomplished under Contract AF 33(657)-10835, BPS No. 5(6399-8219-62405364), sponsored by the Flight Control Division of the Air Force Flight Dynamics Laboratory. The research was performed by Systems Technology, Inc., at both its Hawthorne, California, and Princeton, New Jersey, offices, and, under subcontract, by the Franklin Institute Laboratories for Research and Development, Philadelphia, Pennsylvania. The project principal investigators were Duane McRuer and Dunstan Graham, of STI, and E. S. Krendel, of FIL. The Flight Control Division project engineers have been Capt. J. E. Pruner and P. E. Pietrzak.

Many others besides the authors have contributed to the results reported here. All of the principal investigators participated in the detailed planning and data interpretation phases. A major contribution was made by W. C. Reisener, Jr., of The Franklin Institute, who executed the experiments and data reduction phases. The authors would like to thank M. M. Solow, who was the subject, and Diane Fackenthal, who assisted in the data reduction phase. Finally, the authors would like to thank R. O. Anderson and P. E. Pietrzak of FDCC for their careful review of the report.

The contractor's internal technical report number is STI-TR-134-3.

The manuscript was released by the authors in December 1966 for publication as an RTD Technical Report.

This technical report has been reviewed and is approved.



C. B. WESTBROOK

Chief, Control Criteria Branch
Flight Control Division
AF Flight Dynamics Laboratory

ABSTRACT

The purpose of the experimental efforts reported here is to explore on a preliminary basis the limiting characteristics of the human operator's "actuator" or neuromuscular system dynamics as affected by the manipulator. The effects of three manipulators (pressure, free-moving, and spring-restrained) on system performance and the human operator's describing function are presented for three controlled elements and two high bandwidth forcing functions. Describing function differences are primarily in the phase, i.e., the effective time delay at high-frequency and an effective phase lag at very low frequencies.

Generally the mean square error and describing function results for the spring-restrained manipulator were intermediate to those for the free-moving (no spring) and the pressure (infinite spring) manipulators. The pressure controller gave lower mean square error and less effective time delay than the free-moving controller. In addition, the effective phase lag at very low frequencies was either the same as or larger than that for the free-moving control.

Contrails

Contrails

TABLE OF CONTENTS

	PAGE
I. INTRODUCTION	1
A. Project Background and Purpose	1
B. Outline of the Report	6
II. MEASUREMENT CONDITIONS, FORCING FUNCTIONS, AND EXPERIMENTAL PLAN	7
A. General	7
B. Description of the Forcing Function.	7
C. Description of the Manipulators and Controlled Elements.	11
III. EXPERIMENTAL DATA	15
A. Performance Measure Comparison	15
B. Describing Function Comparison	18
IV. CONCLUSIONS	38
REFERENCES.	39

Contrails

ILLUSTRATIONS

1.	Typical Pilot Describing Function Data and Models; ($Y_c = K_c/(s-2)$; $\omega_1 = 4.0$ rad/sec).	5
2.	General Measurements and Task Variables	8
3.	Measured Forcing Function Power Spectra Magnitudes	9
4.	Stick Manipulator	12
5.	Manipulators	13
6.	Various Manipulators Matrix	16
7.	Comparison of Normalized Root Mean-Squared Errors for Free-Moving and Pressure Manipulators.	17
8.	Averaged Describing Functions for Pressure, Spring- Restrained and Free-Moving Manipulators (B5 Input and $Y_c = 1$)	22
9.	Effects of Manipulator (B5 Input and $Y_c = 1$)	23
10.	Averaged Describing Functions for Pressure, Spring- Restrained and Free-Moving Manipulators (R2.2 Input and $Y_c = 1$)	24
11.	Effects of Manipulators (R2.2 Input and $Y_c = 1$)	25
12.	Averaged Describing Functions for Pressure, Spring- Restrained and Free-Moving Manipulators (B5 Input and $Y_c = 10/s$)	26
13.	Effects of Manipulators (B5 Input and $Y_c = 10/s$)	27
14.	Averaged Describing Functions for Pressure, Spring- Restrained and Free-Moving Manipulators (R2.2 Input and $Y_c = 10/s$)	28
15.	Effects of Manipulators (R2.2 Input and $Y_c = 10/s$)	29
16.	Averaged Describing Functions for Pressure, Spring- Restrained and Free-Moving Manipulators (B5 Input and $Y_c = 5/s^2$)	30
17.	Effects of Manipulators (B5 Input and $Y_c = 5/s^2$)	31

Contrails

FIGURE	PAGE
18. Averaged Describing Functions for Pressure, Spring-Restrained and Free-Moving Manipulators (R2.2 Input and $5/s^2$)	32
19. Effects of Manipulators (R2.2 Input and $Y_c = 5/s^2$)	33
20. Effects of Forcing Function Bandwidth (Pressure Manipulator)	34
21. Effects of Forcing Function Bandwidth (Free-Moving)	35
22. Effects of Forcing Function Bandwidth (Spring-Restrained)	36

TABLES

TABLE	PAGE
I. Amplitude Ratio and Phase Lag Comparisons as a Function of Frequency for Free-Moving, Pressure, and Spring-Restrained Stick Manipulators	20
II. Amplitude Ratio and Phase Lag Comparisons as a Function of Frequency for Free-Moving and Pressure Manipulators	20
III. Amplitude Ratio and Phase Comparisons for Forcing Function Variations	37

Contrails

SYMBOLS

a_T	Threshold value of the indifference threshold nonlinearity
B5	Forcing function designation defined on page 18
$c(t)$	Operator output time function
$e(t)$	Error time function
$F(t)$	Limb-applied force
F	Free-moving manipulator
$i(t)$	Forcing function time function
$j\omega$	Imaginary part of the complex variable, $s = \sigma \pm j\omega$
k	The order of the free s term in Y_c
K_c	Controlled element gain
K_p	Human pilot gain
K_s	Control sensitivity — inches (display)/stick motion
K_T	Gain of indifference threshold describing function
$m(t)$	System output time function
n	$T_R\omega_n/2\pi$ number series used to generate forcing function frequency spacing
P	Pressure manipulator
R2.2	Forcing function designation defined on page 18
s	Complex variable, $s = \sigma \pm j\omega$; Laplace transform variable
S	Spring-restrained manipulator
t	Time
T_I	General lag time constant of human pilot describing function
T_K, T'_K	Lead and lag time constants in precision model of human pilot describing function
T_L	General lead time constant of human pilot describing function
T_N, T_{N_1}	Lag time constants (eqs. 1 and 4)

Contrails

T_R	Run length
Y_c	Controlled element (machine and display) transfer function
Y_p	Pilot describing function
α	Low frequency phase approximation parameter
α_F	α for the free-moving manipulator
α_P	α for the pressure manipulator
ζ_N	Damping ratio of second-order component of the neuromuscular system
σ_i	rms value of the forcing function
σ_T	rms value of input to the indifference-threshold
τ	Pure time delay
τ_e	Effective time delay
τ_F	τ_e for the free-moving manipulator
τ_P	τ_e for the pressure manipulator
φ	Phase angle
φ_i	Peak amplitude of sine wave
ϕ_{ic}	Cross power spectral density between i and c
ϕ_{ie}	Cross power spectral density between i and e
ϕ_{ii}	Forcing function power spectral density
ϕ_{nn}	Closed-loop remnant spectral density, at pilot's output
ω	Angular frequency, rad/sec
ω_c	System crossover frequency, i.e., frequency at which $ Y_p Y_c = 1$
ω_i	Forcing function bandwidth
ω_n	Frequency of forcing function sinusoidal component
ω_N	Undamped natural frequency of second-order part of the neuromuscular system
\doteq	Approximately equal to

Contrails

\angle	Angle of
db	Decibels; $10 \log_{10} $ if a power quantity, e.g., spectrum; $20 \log_{10} $ if an amplitude quantity, e.g., Y_p
$ $	Magnitude
$ _{db}$	Magnitude in db
$(\bar{\quad})$	Mean value
\mathcal{L}^{-1}	Inverse Laplace transform

CHAPTER I INTRODUCTION

A. PROJECT BACKGROUND AND PURPOSE

The investigation reported here is an element in a USAF research program undertaken to explore and exploit the concept that vehicle dynamic handling qualities are to a large extent dependent on the action of the pilot as a control element. This concept is based on the methods of control engineering and treats the pilot/vehicle system as a closed-loop (in general, a multiloop) entity. The sine qua non of the handling quality or, more generally, the man/machine control theory is a model of the pilot dynamic characteristics expressed in a form suitable for application using relatively conventional control engineering techniques. Serviceable but incomplete models have been evolved from a data base built up over the last 25 years (Refs. 9-11, 14, 16, 17, 19, 20, 21, 23-25, 32, 34, 35, 41) which has been substantially expanded recently by a companion report (Ref. 27) to the present work. The models derived from this data base have at each stage in their evolution been extensively applied in handling qualities and pilot/vehicle system analysis (Refs. 1-4, 6-8, 12, 18, 22, 31, 33, 37, 38, 39, 40). The success of such applications has increased the importance of a more complete understanding of the mathematically describable aspects of human dynamics in vehicle control systems. Because the applications of the theory are limited fundamentally by the level of pilot model knowledge, which is in turn dependent on the data base, new data of increased scope and precision are required. Some of these needs are met by Ref. 27, while others are treated here.

The experimental efforts reported here were undertaken to explore on a preliminary basis the limiting characteristics of the human pilot's "actuator" or neuromuscular system dynamics as affected by the manipulator. Before the current and the Ref. 27 experimental series, the available random-input describing function data usually did not extend to high enough frequencies to exhibit much about about the neuromuscular system

Contrails

dynamics (a few exceptions are given in Ref. 9). In fact, although the previous data involved experiments with manipulators as varied as aircraft control sticks, hand wheels, spade grips, and a pencil-like stylus, comparison of the results indicated that the influence of the manipulator was unimportant for the frequency ranges measured and manipulators tested. The describing function data did, however, reflect the mid-frequency effects of the high frequency neuromuscular system. They required a first-order lag as a minimum first approximation to the neuromuscular system, and this lag has commonly been the highest frequency term in the pilot's describing function form.

The frequency range over which accurate pilot describing function measurements can be obtained has been considerably extended in the current series of experiments, so the actuator characteristics as an element in the total describing function are now far better reflected by the describing function data. For instance, the so-called precision model, which is the most general describing function model form given by Ref. 27, contains many actuator elements. Its form is

$$Y_p(j\omega) = K_p K_T \left(\frac{a_T}{\sigma_T} \right) e^{-j\omega\tau} \left(\frac{T_L j\omega + 1}{T_I j\omega + 1} \right) \left(\frac{T_K j\omega + 1}{T'_K j\omega + 1} \right) \left[\frac{1}{(T_{N1} j\omega + 1) \left[\left(\frac{j\omega}{\omega_N} \right)^2 + \frac{2\zeta_N}{\omega_N} j\omega + 1 \right]} \right] \quad (1)$$

where K_p = gain

$K_T \left(\frac{a_T}{\sigma_T} \right)$ = indifference threshold describing function

$\frac{T_L j\omega + 1}{T_I j\omega + 1}$ = equalization characteristic; T_L and T_I values depend on form of controlled element

$e^{-j\omega\tau}$ = fixed time delay due to conduction times of various subsystem elements

$\frac{T_K j\omega + 1}{T'_K j\omega + 1}$ = terms which are used to describe very low frequency phase data

$\frac{1}{(T_{N1} j\omega + 1) \left[\left(\frac{j\omega}{\omega_N} \right)^2 + \frac{2\zeta_N}{\omega_N} j\omega + 1 \right]}$ = neuromuscular system elements

Contrails

The describing function is written in terms of the frequency operator, $j\omega$, instead of the Laplace transform variable, s , to emphasize that this describing function is only valid in the frequency domain and only exists under essentially stationary conditions. For instance, it cannot be used to compute the system response to a discrete input, e.g., a step response, although some of the terms in the model may be compatible with step response data.

The major elements of complication introduced in this precision model are those in the braces. These all appear to arise from the neuromuscular system, which has both very high and very low frequency effects.

The very low frequency characteristics appear in the data primarily as a phase lag. In the precision model these characteristics are represented by the lead/lag, $(T_K j\omega + 1)/(T_K' j\omega + 1)$, which is a minimum form suitable to characterize both amplitude ratio and phase data completely. For many systems these low frequency effects can be further approximated, as derived below, by the single-parameter form $e^{-j\alpha/\omega}$. If the low frequency effects are modeled by transfer characteristics containing m lags and leads, then the incremental phase shift due to these will be

$$\Delta\phi_{\text{low}} = \sum_{i=1}^m \tan^{-1} \omega T_{\text{lead}_i} - \sum_{i=1}^m \tan^{-1} \omega T_{\text{lag}_i} \quad (2)$$

At frequencies well above the break frequencies of these lags and leads, i.e., $\omega > 1/T_{\text{lead}_i}, 1/T_{\text{lag}_i}$, this can be approximated by

$$\begin{aligned} \Delta\phi_{\text{low}} &\doteq \sum_{i=1}^m \left(\frac{\pi}{2} - \frac{1}{\omega T_{\text{lead}_i}} \right) - \sum_{i=1}^m \left(\frac{\pi}{2} - \frac{1}{\omega T_{\text{lag}_i}} \right) \\ &\doteq \frac{1}{\omega} \sum_{i=1}^m \left(\frac{1}{T_{\text{lag}_i}} - \frac{1}{T_{\text{lead}_i}} \right) \\ &\doteq -\left(\frac{\alpha}{\omega} \right) \end{aligned} \quad (3)$$

Thus, $e^{-j\alpha/\omega}$ is seen to be an approximation for the mid-frequency effects of very low frequency leads and lags. It is suitable to describe much

Contrails

of the very low frequency phase lag, although it cannot account for the magnitude effects of the lag/lead since its amplitude ratio is 1.

The high frequency neuromuscular system characteristics are represented by the third-order denominator in the precision model, whereas mid-frequency approximations to the high frequency effects are suitable for the approximate model. These may be either a first-order lag (so-called neuromuscular lag) or a pure time delay. Combining both the low and high frequency approximations to the precision model neuromuscular system characteristics yields

$$\left(\frac{T_K j\omega + 1}{T'_K j\omega + 1} \right) \left\{ \frac{1}{(T_{N1} j\omega + 1) \left[\left(\frac{j\omega}{\omega_N} \right)^2 + \left(\frac{2\zeta_N}{\omega_N} \right) j\omega + 1 \right]} \right\} \doteq \frac{e^{-j\alpha/\omega}}{T_N j\omega + 1} \quad \text{or} \quad e^{-j(\alpha/\omega + T_N \omega)} \quad (4)$$

where $\alpha \doteq \frac{1}{T_K} - \frac{1}{T'_K}$, $T_N \doteq T_{N1} + \frac{2\zeta_N}{\omega_N}$

Thus, the approximate pilot model in the mid-band region becomes

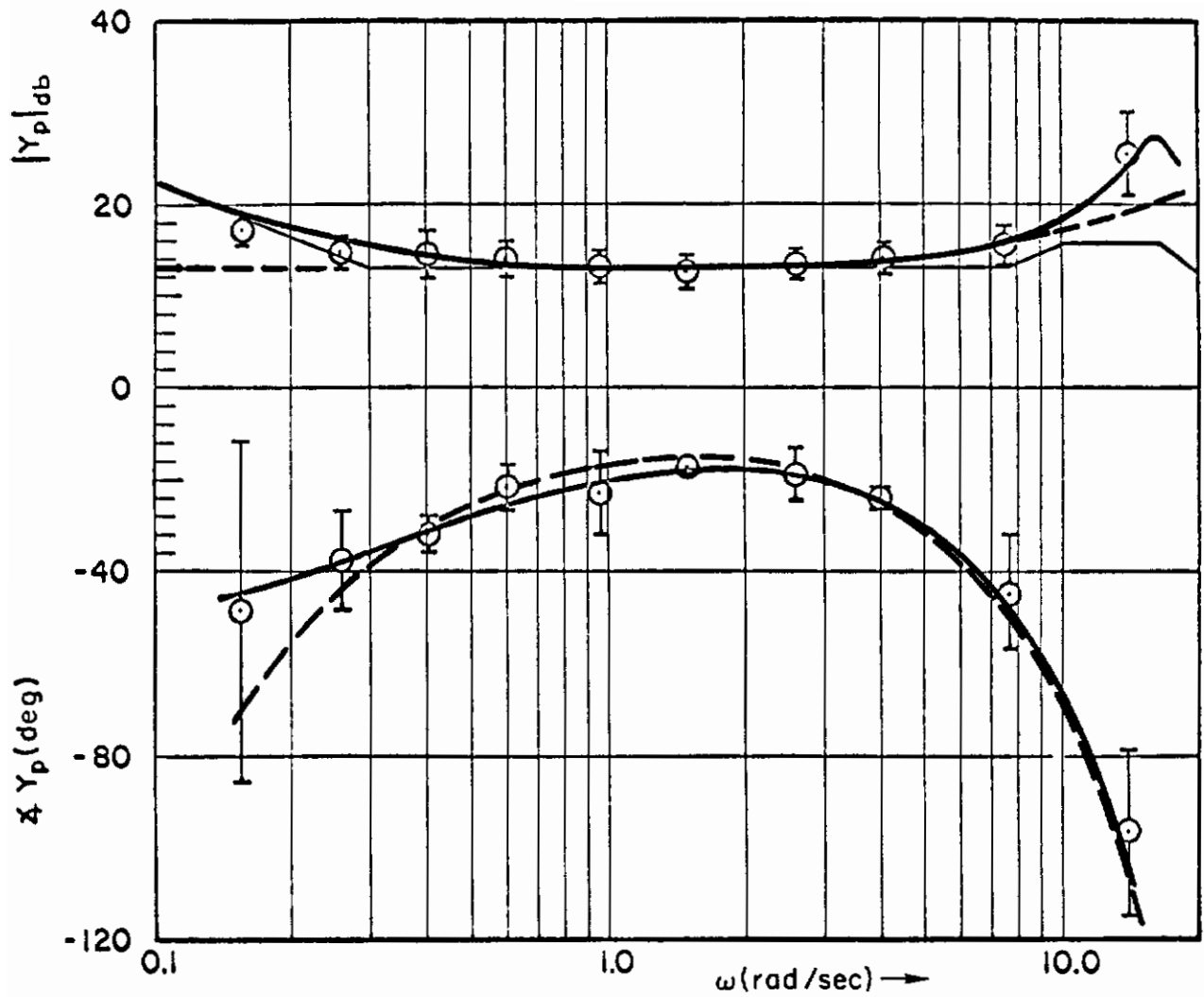
$$Y_p(j\omega) = K_p \underbrace{\left(\frac{T_L j\omega + 1}{T_I j\omega + 1} \right)}_{\substack{\text{Gain, including} \\ \text{indifference} \\ \text{threshold and} \\ \text{the ratio } T_K/T'_K}} e^{-j(\alpha/\omega + T_N \omega + \tau\omega)} \quad (5)$$

Equaliza-
tion, form
depends
on $Y_c(s)$
High and low
frequency
approximation
to neuromuscular
system

In this report we shall deal primarily with the α and T_N approximations to the neuromuscular system rather than with its finer details.

Some appreciation for the adequacy of approximations described is given in Fig. 1. This shows typical pilot describing function data and both the precision and approximate model forms as descriptors of these data. These data are from a so-called subcritical task in which the controlled element consists of a first-order divergence (Ref. 27). Because the $e^{-j(\alpha/\omega + T_N \omega)}$ approximation does not affect the amplitude ratio, the very highest and very lowest frequency amplitude ratio points are

Contrails



Precision Model (—)

$$Y_p = (25.1) \left(\frac{j\omega}{7.8} + 1 \right) e^{-0.09j\omega} \left\{ \frac{\left(\frac{j\omega}{0.3} + 1 \right)}{\left(\frac{j\omega}{0.05} + 1 \right)} \frac{1}{\left(\frac{j\omega}{10} + 1 \right) \left[\left(\frac{j\omega}{16.5} \right)^2 + \frac{2(0.12)}{16.5} j\omega + 1 \right]} \right\}$$

Approximate Model (---)

$$Y_p = (4.2) \left(\frac{j\omega}{7.8} + 1 \right) e^{-j[0.21\omega + (0.19/\omega)]}$$

Figure 1. Typical Pilot Describing Function Data and Models
 ($Y_c = K_c/(s - 2)$; $\omega_1 = 4.0$ rad/sec)

Conclusions

not adequately described by the approximation, which is otherwise quite good. Note that the gain in the approximate model is related to the low frequency gain of the precision model by the ratio T_K/T_K' or 0.05/0.3. In the particular example given in Fig. 1 the two fits use a different α —the smaller value used in the approximate model yields a better fit to the data at lower frequencies. The joint action of the $T_N\omega$ and α/ω phase lages tend to make the phase look like an umbrella, with α controlling the left and T_N the right portion. That is, changes in T_N distort the right side of the umbrella, while changes in α shift the left. Simultaneous increases or decreases in both α and $1/T_N$ shift the umbrella to the right or left, respectively.

The Ref. 27 experimental series was concerned primarily with the effects on pilot dynamics of forcing function and controlled element variations with constant manipulator characteristics. The current series expands on these measurements by introducing the dimension of manipulator variation. Specifically, the limiting cases of unrestrained or free-moving and essentially rigid pressure-actuated manipulators are studied. These exploratory efforts reveal distinct differences between the describing functions adopted by the operator, especially in the neuromuscular characteristics as described by α and T_N . This new knowledge should have significant impact on the design of manipulative devices with which the pilot imparts his desires to the vehicle.

B. OUTLINE OF THE REPORT

The preceding portions of Chapter I discussed a first-order approximation of the neuromuscular system which appears to have both very high and very low frequency phase effects. The data to be presented will be discussed in terms of the parameters τ_e (which describes the high frequency phase) and α (which describes the very low frequency phase).

Chapter II describes the experimental configuration, forcing function, manipulators, and controlled elements.

Chapter III presents the performance measure and describing function results. Comparison plots illustrate the differences between the pressure, free-moving and spring-restrained manipulators. Additional comparisons indicate the effects of forcing function bandwidth.

Finally, Chapter IV summarizes the general conclusions and findings of the study.

CHAPTER II

MEASUREMENT CONDITIONS, FORCING FUNCTIONS, AND EXPERIMENTAL PLAN

A. GENERAL

The experimental portions of this study were intended to make explicit and to quantify aspects of human adaptive behavior which can be demonstrated by considering several different experimental situations, each of which is essentially stationary. Great emphasis was placed on the isolation and control of sources of variability so that the experimental findings could be presented, insofar as possible, in a deterministic rather than statistical fashion. This was accomplished by precise measurements; by using specially contrived experimental and measurement procedures; and by paying meticulous attention to details. These means have been successful enough to allow definitive results to be obtained using a restricted number of experimental runs. A general description of the physical layout and the analysis equipment used is given in Ref. 27.

The task variables and general measurements involved in the experiments are summarized in Fig. 2. The task variables under the experimenter's control are enclosed in dashed boxes comprising the forcing function, $i(t)$, controlled element, Y_C , and manipulator. All three were actually varied in this experimental series.

From the measurable signals in the control loop, two quantities were obtained. These were the average performance of the closed-loop system, as measured by $\overline{e^2}$, and a characterization of the operator transfer dynamics, as indicated by the describing function $Y_p(j\omega)$.

B. DESCRIPTION OF THE FORCING FUNCTION

The forcing function, $i(t)$, is made up of ten sinusoids. The individual waves are so arranged that the composite pattern is random appearing to insure that the operator cannot detect any internal coherence in the forcing function and thereby adopt a higher level of behavior. The amplitude distribution of the forcing function is approximately Gaussian.

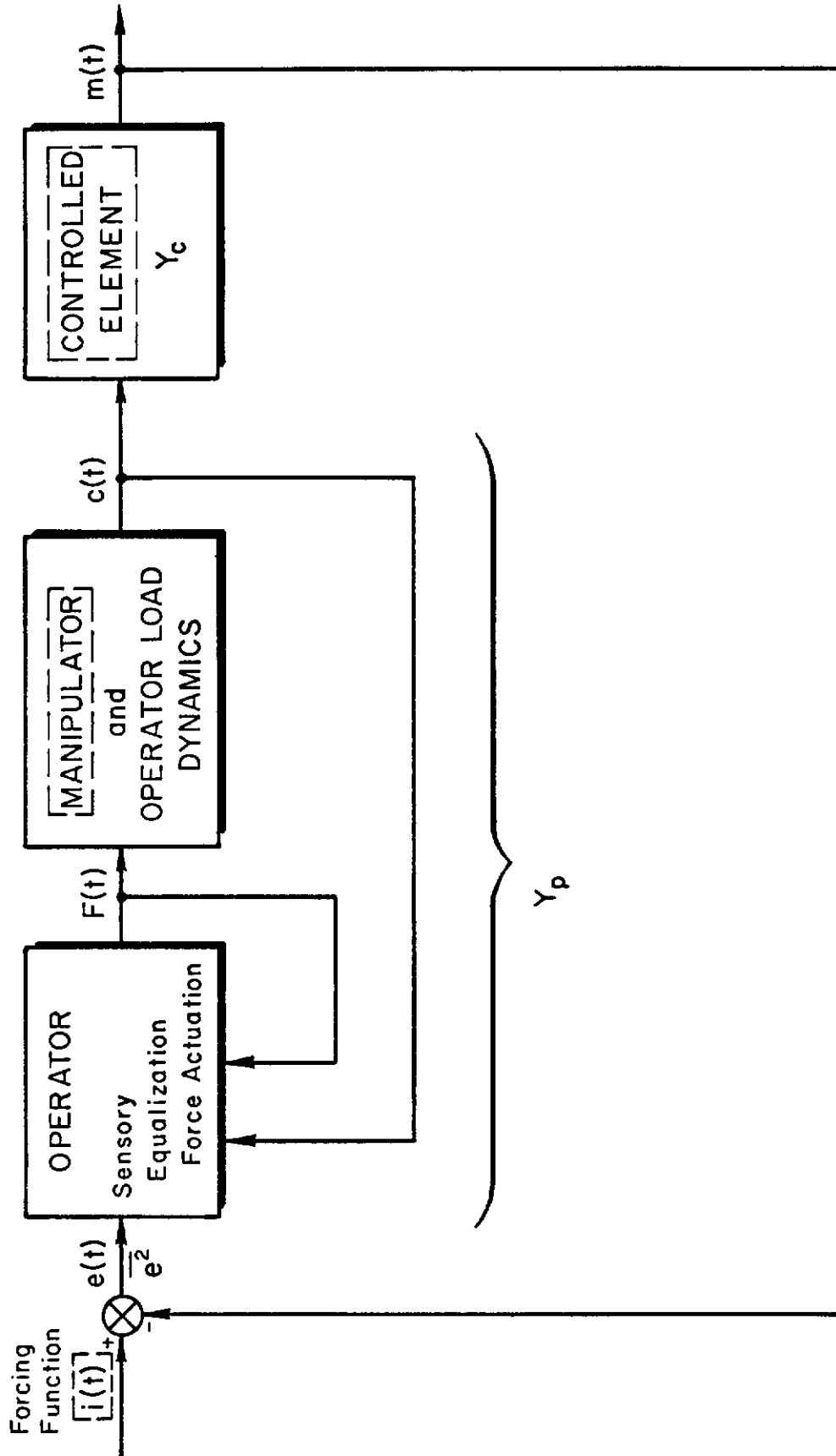


Figure 2. General Measurements and Task Variables

Contrails

A prime factor to be considered in the selection of forcing function frequencies and amplitudes is those features of human behavior which are to receive emphasis in the measurement program. In this study the high frequency characteristics of the operator were central. This emphasis made it desirable to have as much power as possible in the higher frequencies, in an attempt to improve accuracy and definition. But if the high frequency power is too great, the operator will tend to behave in a manner drastically different from that exhibited in Ref. 27 and elsewhere. For instance, in Ref. 9 extremely broad band forcing functions, R1.6 and R2.4, evoked behavioral characteristics which differed in their very nature from those obtained with much lower bandwidth forcing functions. Taking such past data into account, two forcing function spectra were selected. By analogy with Ref. 9 these were called R2.2 (which was an approximation to a broad band rectangular spectrum with cutoff at about 2.2 cycles per second) and B5 (which was an input similar to the augmented rectangular spectra used in Ref. 27, except that the high frequency shelf was 10 db down from the low frequency amplitudes rather than 20 db). Measured forcing function power spectra magnitudes for these are shown in Fig. 3.

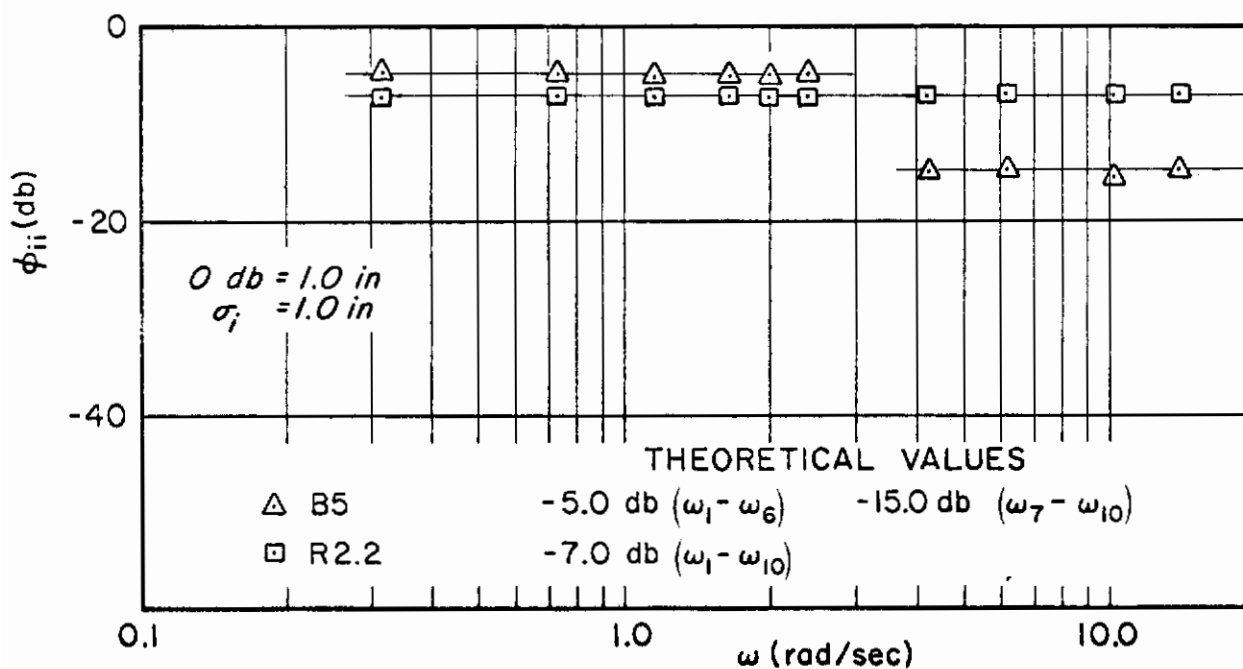


Figure 3. Measured Forcing Function Power Spectra Magnitudes

Contrails

The specific values of the frequencies in radians per second are listed below along with the number of cycles per minute. The latter clearly indicates that the input frequencies are not harmonically related, thus insuring the random appearance of the input.

<u>ω_n (rad/sec)</u>	<u>n</u>
0.314	3
0.732	7
1.151	11
1.675	16
1.989	19
2.407	23
4.29	41
6.17	59
10.14	97
14.03	134

The sine wave at 10.14 rad/sec was inadvertently set to 7.5 rad/sec for the free-moving control with $Y_c = K_c/s^2$.

C. DESCRIPTION OF THE MANIPULATORS AND CONTROLLED ELEMENTS

The controlled elements used had the three simple forms K_c , K_c/s , and K_c/s^2 . They were generated with analog circuits which received as input the pilot's manipulator output. The controlled element output was subtracted from the forcing function to create a system error which was presented on a cathode ray oscilloscope display. The general experimental arrangement with one of the manipulators used is shown in Fig. 4. Typically, the eye-to-scope distance was about 29 inches.

The three kinds of manipulators used are shown in Fig. 5. The first was the sidestick previously used in Ref. 27. This is spring-restrained and is designed to exhibit minimum possible inertia, damping, and nonlinearities. Its basic characteristic was a force of 2.2 ounces

Contrails

per degree of stick on a 4-inch moment arm (8.8 inch-ounces per degree of spring restraint). The display and controlled element circuit gains were set to give a deflection sensitivity on the display for a $Y_C = K_C = 1.0$ controlled element as follows:

$$\begin{aligned} K_S &= 0.167 \text{ in. (display)/degree (stick)} \\ \text{or} \quad K_S &= 2.38 \text{ in. (display)/per inch (stick)} \\ K_S &= 0.0754 \text{ in. (display)/per ounce (stick)} \end{aligned}$$

The second manipulator consisted of a knob located near the periphery of a wheel. The control was operated with the same sort of lateral motion as used with the stick. The wheel was unrestrained and nearly frictionless, and consequently approximated a free-moving control. Circuit gains were set such that for a $Y_C = K_C = 1.0$ controlled element the display sensitivity was

$$K_S = 1 \text{ in. (display)/in. (knob)}$$

The third manipulator used the same adjustable arm rest mount as the free-moving control, but with a rigid lever with strain gauge pickup substituted for the wheel. Forces were applied to this lever for pressure control by the same muscle group as was used in the free-moving control. The display sensitivity for the pressure controller with a pure-gain controlled element was

$$K_S = 0.067 \text{ in. (display)/ounce (lever)}$$

The lever was 4 inches long.

For frequency-dependent controlled elements the dynamics of the controlled element intervene between the manipulator output and the display. The deflection sensitivities, when referred to the display as a common point, then become dynamic entities. For example, with a unit step displacement of 1 deg applied to the stick, the deflection on the scope will be $0.167 \mathcal{L}^{-1}(Y_C/s)$ if this convention is used.

For convenience and simplicity it is much easier to think of the deflection sensitivities in terms of the steady-state characteristics which are ultimately approached after a unit manipulator deflection. For this type of description the appropriate expressions for the stick are

Controls

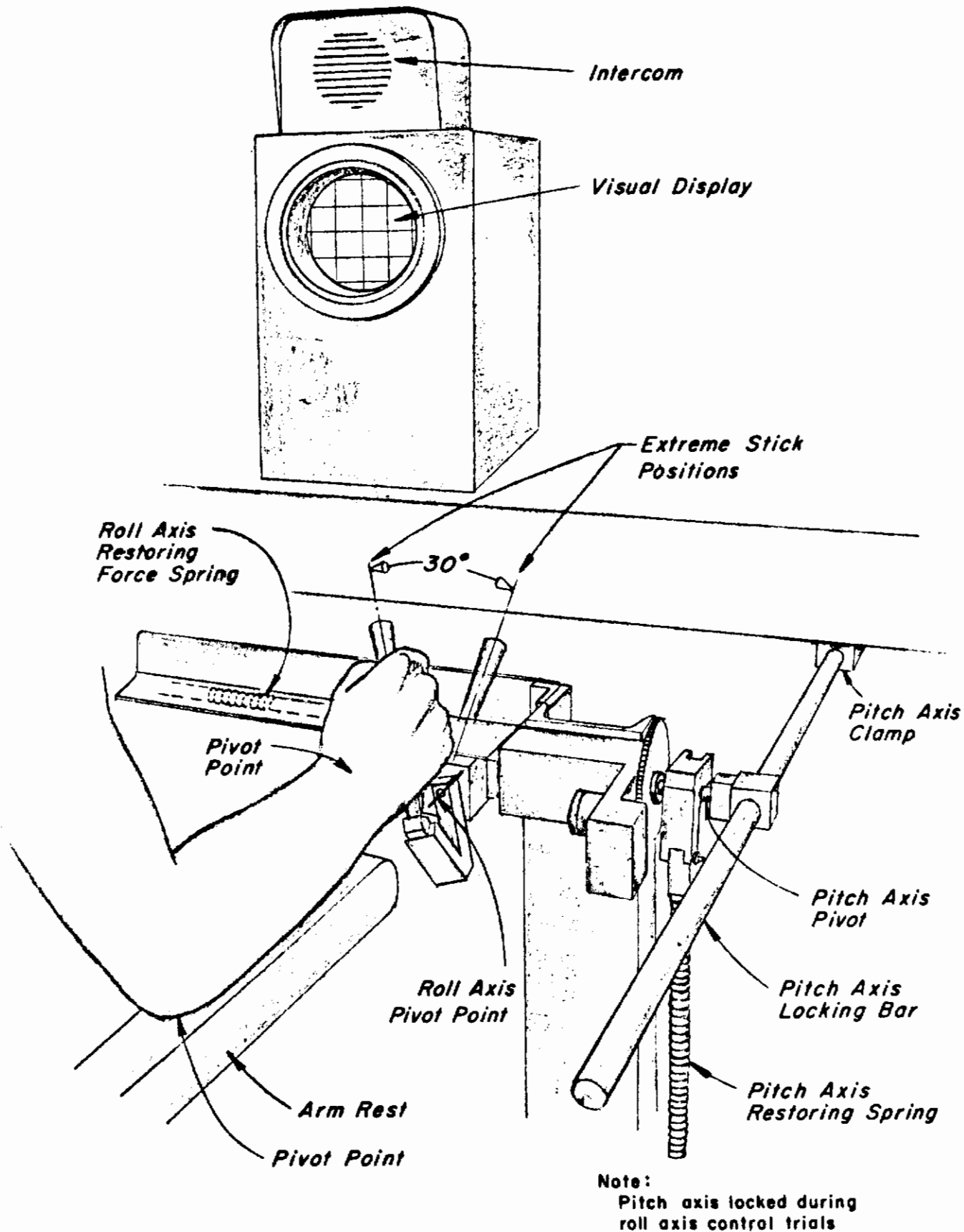
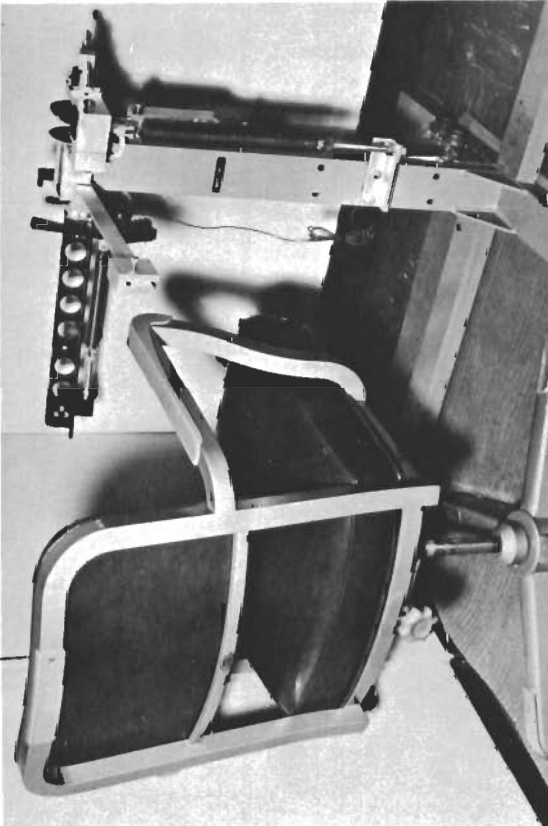
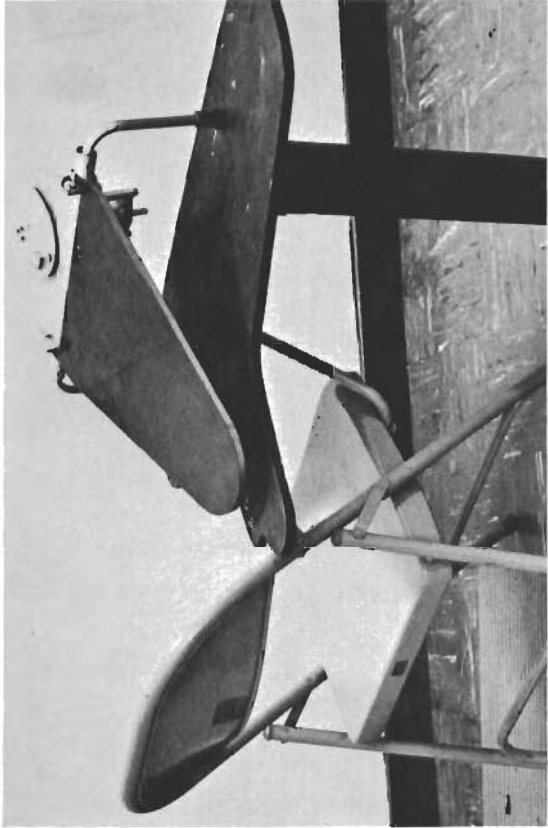


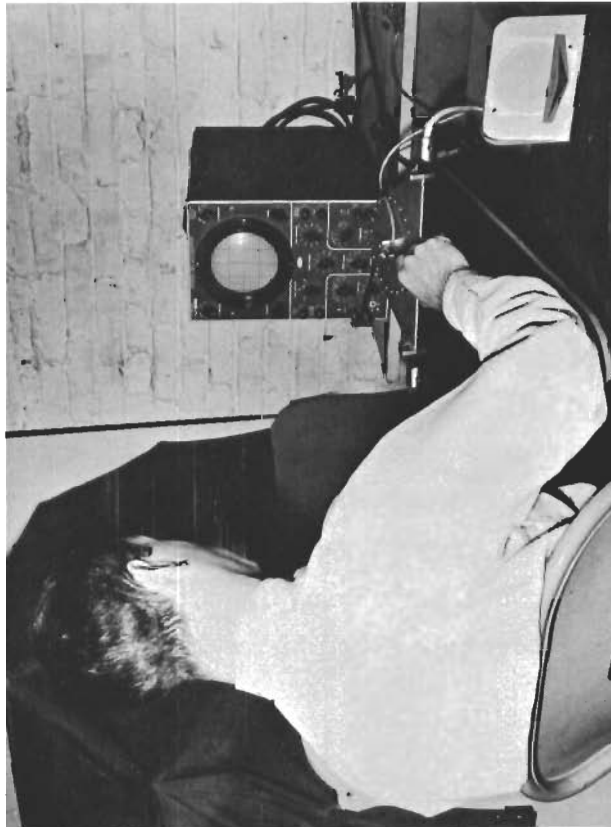
FIGURE 4. STICK MANIPULATOR



SPRING-RESTRAINED CONTROLLER



FREE-MOVING CONTROLLER



PRESSURE CONTROLLER

Figure 5. Manipulators

Contraails

$$K_S = 0.167 \left[s^k Y_C(s) \right]_{s=0} \text{ in./deg}$$

$$K_S = 2.38 \left[s^k Y_C(s) \right]_{s=0} \text{ in./in.}$$

$$K_S = 0.0754 \left[s^k Y_C(s) \right]_{s=0} \text{ in./oz}$$

where k is the order of the free s term in Y_C

For example, if $Y_C = K_C/s$, the deflection sensitivity will be $0.167K_C$ in./sec (display)/deg (stick). The dynamic sensitivities for the other manipulators are similarly defined.

The data reduction apparatus was the watt-hour meter analyzer and associated equipment described in Ref. 27. Extensive tests on this equipment indicate an accuracy for the describing function measurements of about 0.5 db in amplitude and 4° in phase over a dynamic range greater than 40 db in amplitude and 2 decades in frequency.

The computation time for the experiment was accurately controlled, equal to an integral number of periods of the input frequencies, with a typical run length of 4 min. Prior to the beginning of the computation, 10 to 15 sec were allowed for the operator to reach a stable tracking condition. Before and after each experiment, the readings of the watt-hour meters were recorded. Three of these were used to measure $\overline{i^2}$, $\overline{e^2}$, and $\overline{c^2}$, and 40 others to measure cross-spectral components. From the latter the operator's describing function was calculated at each of the input frequencies, ω_n , using the relationship

$$Y_p(j\omega_n) = \frac{\Phi_{ic}(j\omega_n)}{\Phi_{ie}(j\omega_n)} \quad (6)$$

CHAPTER III

EXPERIMENTAL DATA

This chapter presents the performance measure and describing function data obtained to investigate the effects of the various manipulators discussed in Chapter II. Emphasis is placed on the high and low frequency ends of the pilot's describing function as indicators of neuromuscular system effects.

The experimental matrix, Fig. 6a, shows the combinations of manipulator, controlled element, and forcing function used. The crosses in Fig. 6b indicate that different rms input sizes were used for various controlled-element/forcing-function combinations. At least three replications were performed, with as many as six for the $Y_c = 5/s^2$, R2.2 cases. The latter case, being the most difficult to control, had the largest variability. The additional runs enabled a better estimate of the underlying average describing functions and performance to be made.

The subject was a light-airplane-qualified civilian pilot with extensive tracking experience who has participated in all Systems Technology, Inc./Franklin Institute Laboratory experiments. Because of this extensive experience the subject was able to rapidly approach asymptotic values of performance, thereby permitting a large number of configurations to be examined at minimal cost. While more subjects would have been desirable, the exploratory and limited-effort nature of the experimental series made this unrealistic. In Ref. 27 he is shown to be representative of a population of pilots, whereas in Refs. 26 and 30 he is the sole subject.

A. PERFORMANCE MEASURE COMPARISON

The effect of the manipulator on performance is given in Fig. 7 for the limiting cases of pressure and free-moving controllers. Except for $Y_c = K_c/s$, R2.2 input, the RMS error for pressure control is smaller than that for the free-moving control. This result correlates with

Y _c	MANIPULATOR	FORCING FUNCTION					
		B5		R2.2			
		.5"	1"	.25"	.5"	1"	1"
Acceleration Control 5/s ²	Spring - Restrained	X			X		
	Pressure	X			X		
	Free - Moving	X			X		
Velocity Control 10/s	Spring - Restrained	X				X	
	Pressure	X				X	
	Free - Moving	X				X	
Displacement Control 1	Spring - Restrained					X	X
	Pressure					X	X
	Free - Moving					X	X

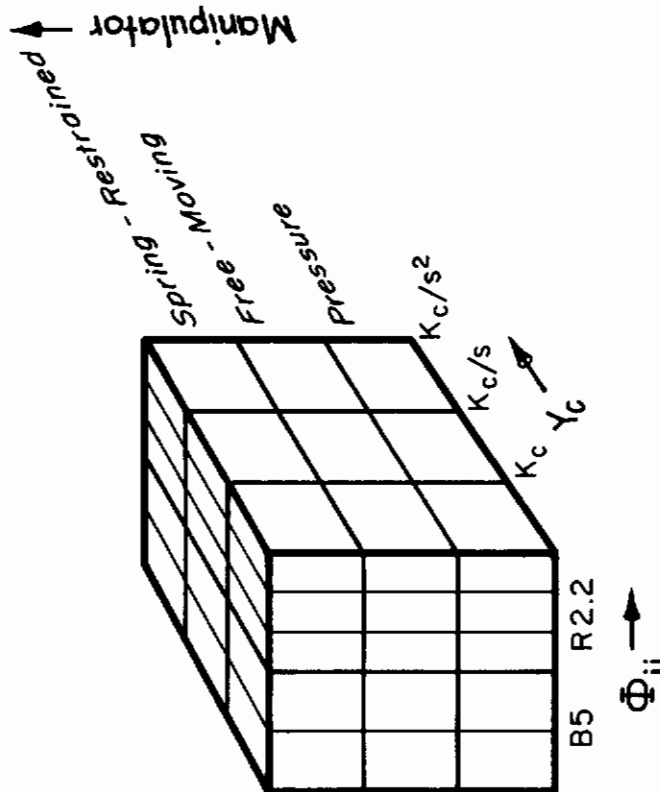


Figure 6. Various Manipulators Matrix

Y_c	B5	R2.2
K_c	○	⊙
K_c/s	△	⊠
K_c/s^2	□	⊞

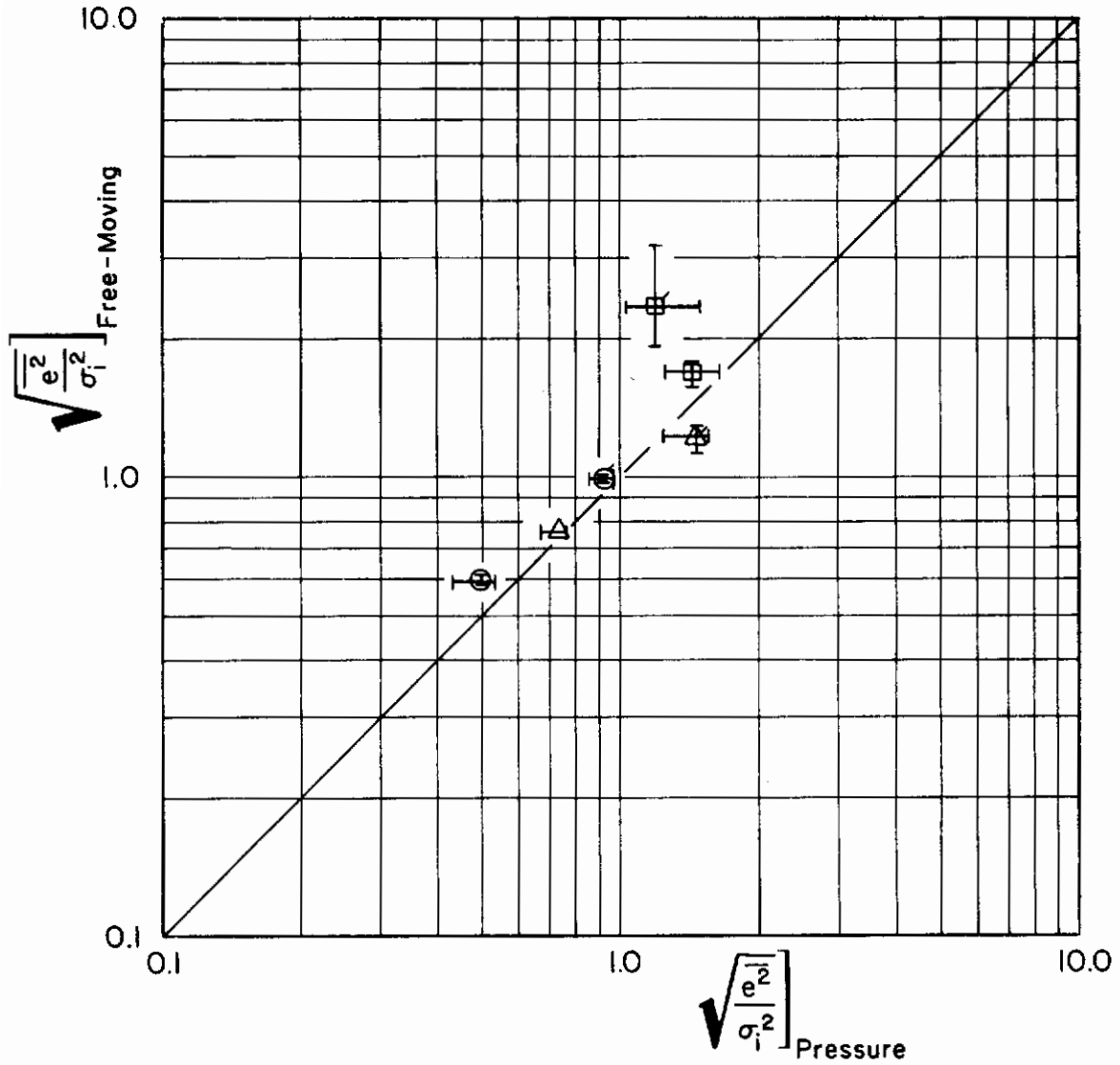


Figure 7. Comparison of Normalized Root Mean-Square Errors for Free-Moving and Pressure Manipulators

the results in Ref. 13 for these two manipulator types. There it was found that the pressure control, which was superior to the free-moving control for all conditions, appeared to greatest advantage when it was being relaxed toward center under the influence of its spring restraint (i.e., when the input had a negative acceleration), and also when the input reversed (changed direction). The free-moving controller had larger tracking errors at these reversal points because there was a sudden change in the direction of the input motion, requiring a corresponding change in the continuous tracking adjustments of the limb.

B. DESCRIBING FUNCTION COMPARISON

This section presents the describing function data comparisons to show the effects of manipulator and forcing function on the high and low frequency regions, with emphasis on the implications for the describing function terms α and T_N discussed in Chapter I.

The data are presented in open-loop form, i.e., $Y_p Y_C(j\omega)$, which in the crossover region becomes approximately

$$Y_p Y_C(j\omega) = \frac{\omega_c e^{-j(\tau_e \omega + \alpha/\omega)}}{j\omega} \quad (7)$$

where the pilot's equalization, Eq. 5, has been selected so that the open-loop amplitude ratio has approximately a -20 db/decade slope in the crossover region, i.e., a low frequency lag is selected for $Y_C = K_C$ and a low frequency lead for $Y_C = K_C/s^2$, while neither is needed for $Y_C = K_C/s$. In Eq. 7 there is a clear separation of phase and amplitude ratio effects, with the high frequency phase effects described by τ_e , the effective time delay, and the low frequency phase effects by α .

1. Effects of Manipulator

The describing function data are presented in Figs. 8-19. Results for the three manipulators on each of the six configurations (three controlled elements and two inputs) are plotted separately (mean data with

Contrails

the variance indicated by hatch marks) and in comparison plots (mean data only).

Qualitative comparisons of the pressure (P) free-moving (F) and spring-restrained (S) manipulators (Table I) are given in terms of amplitude ratio and phase lag in the low, middle (near crossover), and high frequency regions. The entries in the boxes indicate which manipulator had the largest value of the quantity given at the top of each column. When there are two quantities on the left side of the 'greater than' sign (>) it means that the two quantities are approximately equal and both are greater than that on the right side. The purpose of Table I is primarily to indicate that the spring-restrained describing function results are generally intermediate between or the same as those for the pressure and free-moving controllers. This is a reasonable result since the spring-restrained manipulator is intermediate between the infinite spring (pressure) and no spring (free-moving) controllers.

The primary data of interest are those for the two limiting cases, pressure controller and free-moving controller. These comparisons are given in Table II, where the type of shading indicates which manipulator had the largest amplitude ratio or phase lag in the various frequency ranges. A general comment is that the free-moving manipulator consistently has more phase lag at high frequencies than does the pressure controller, whereas the amount of phase lag at low frequency is either the same or larger for the pressure controller. For $Y_C = K_C/s^2$ the pressure controller has a much larger amplitude ratio at high frequencies than does the free-moving controller.

Detailed comments are, using subscripts, "P" (pressure) and "F" (free-moving), and using either τ_F or τ_P for the effective time delay:

$$\underline{Y_C = K_C}$$

The high frequency amplitude ratio is the same for all inputs, therefore the phase differences imply that $\tau_F > \tau_P$. The low frequency amplitude ratio and phase lag are the same for the B5 input, implying that $\alpha_P \doteq \alpha_F$. For the R2.2 input there are slight differences in amplitude ratio trends at mid-frequencies which tend to account for the small phase

Contrails

TABLE I

AMPLITUDE RATIO AND PHASE LAG COMPARISONS AS A FUNCTION OF FREQUENCY FOR
FREE-MOVING, PRESSURE, AND SPRING-RESTRAINED STICK MANIPULATORS

CONTROLLED ELEMENT	FORCING FUNCTION	AMPLITUDE RATIO			PHASE LAG		
		LOW	MID	HIGH	LOW	MID	HIGH
K_c	B5						F > S > P
	R2.2		F, S > P		P > F, S		F > S > P
$\frac{K_c}{s}$	B5				P > F, S		F, P > S
	R2.2		P > F, S		P > F, S		F > P, S
$\frac{K_c}{s^2}$	B5			P > F > S			F > S > P
	R2.2			P > F, S			F > P, S

Blank space indicates F = P = S

TABLE II

AMPLITUDE RATIO AND PHASE LAG COMPARISONS AS A FUNCTION OF FREQUENCY FOR
FREE-MOVING AND PRESSURE MANIPULATORS

CONTROLLED ELEMENT	FORCING FUNCTION	AMPLITUDE RATIO			PHASE LAG		
		LOW	MID	HIGH	LOW	MID	HIGH
K_c	B5						
	R2.2						
$\frac{K_c}{s}$	B5						
	R2.2						
$\frac{K_c}{s^2}$	B5						
	R2.2						

P = F

F > P

P > F

differences such that $\alpha_P \doteq \alpha_F$ for this case also. The magnitude of the α 's required can be obtained with a single lag/lead. In addition, a first-order lead at high frequency is indicated by the amplitude ratio data. Note that the pilot exhibits ω_c regression for the R2.2 input for both controllers. The effect of these trends on the RMS error is that the lower effective time delay for P should lead to a lower error score. For R2.2 this is offset somewhat by the reduced mid-band gain.

$$\underline{Y_C = K_C/s}$$

In general, the amplitude ratios are sufficiently similar that the high frequency phase differences can be described by $\tau_F > \tau_P$ and the low frequency phase differences by $\alpha_P > \alpha_F$. The R2.2 input case is regressive for the free-moving controller, while it is not for the pressure controller. The combination of high gain and larger phase lag for the pressure controller results in $\overline{e^2/\sigma_i^2}|_P > \overline{e^2/\sigma_i^2}|_F$ (Fig. 7). About three first-order lag/lead combinations are needed to account for α_P for R2.2, while one or two will do for α_P and α_F for B5.

$$\underline{Y_C = K_C/s^2}$$

Here there are significant amplitude ratio break frequencies just above crossover. An approximate calculation of the resulting phase effects (using the Bode amplitude/phase relations in Ref. 5) revealed that the residual phase implies that $\tau_F > \tau_P$. A qualitative comparison of the low frequency phase data in light of the amplitude ratio data indicates that $\alpha_P \doteq \alpha_F$.

2. Effects of Forcing Function Bandwidth

The data in Figs. 8-19 are cross-plotted in Figs. 20-22 to show the effects of forcing function bandwidth on the open-loop describing functions for the three manipulators on each controlled element. Amplitude ratio and phase comparisons are given in Table III, page 37, for the limiting cases of pressure and free-moving controllers.

The trends are not too clear due to the regressive configurations. Excluding these cases, an increase in the input bandwidth causes an increase in α for the pressure controller, but not for the free-moving controller.

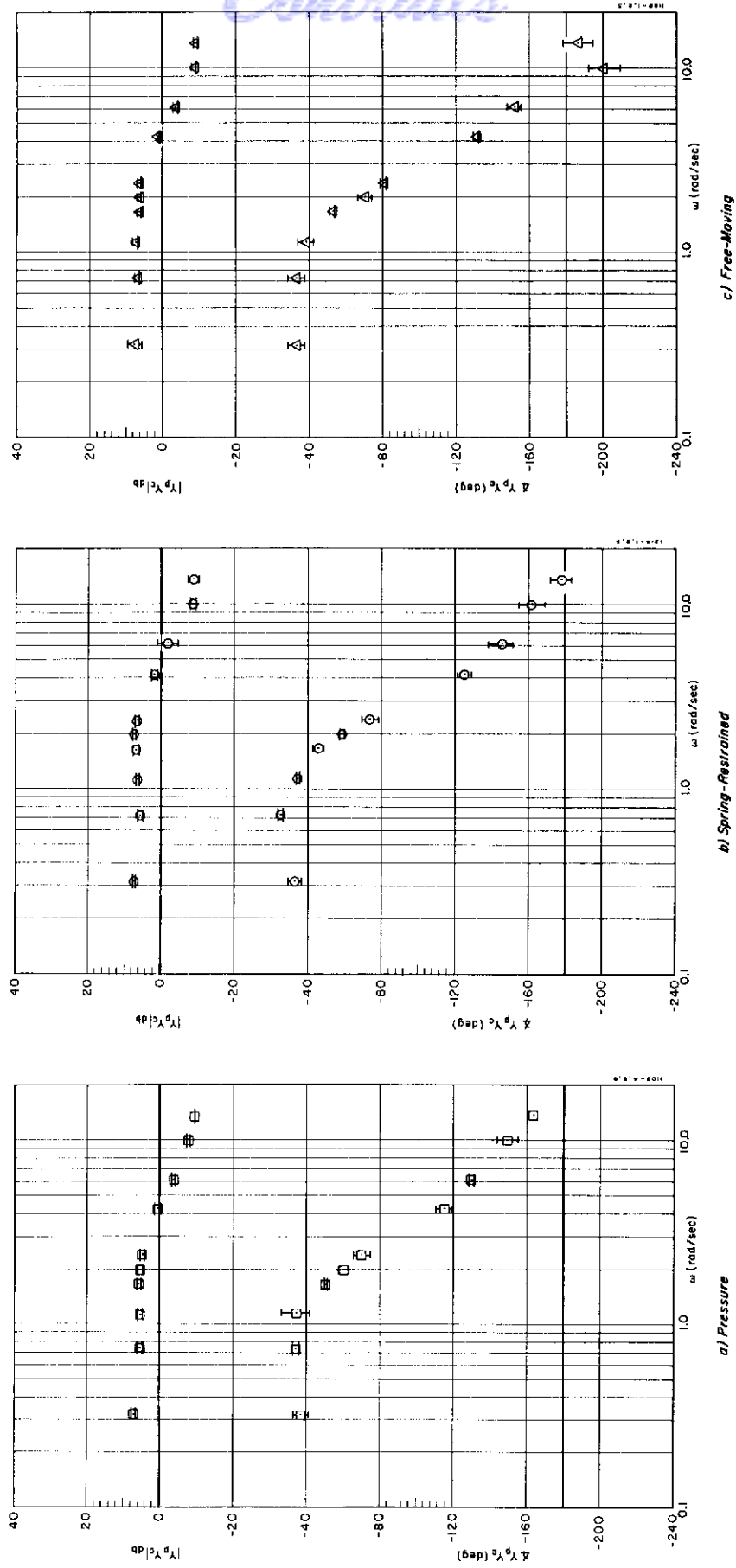


Figure 8. Averaged Describing Functions for Pressure, Spring-Restrained and Free-Moving Manipulators (B_5 input and $Y_c = 1$)

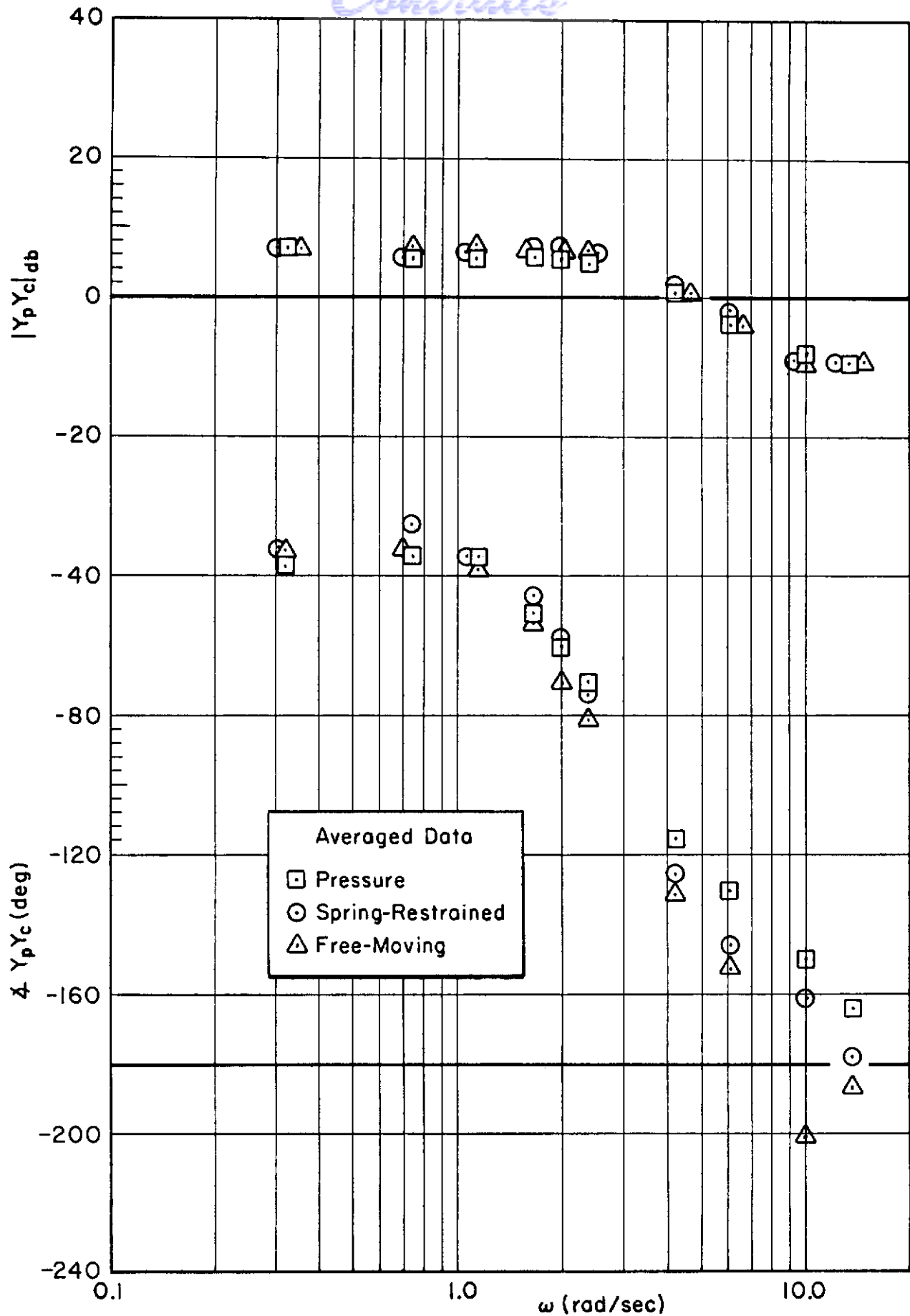


Figure 9. Effects of Manipulator (B5 Input and $Y_c = 1$)

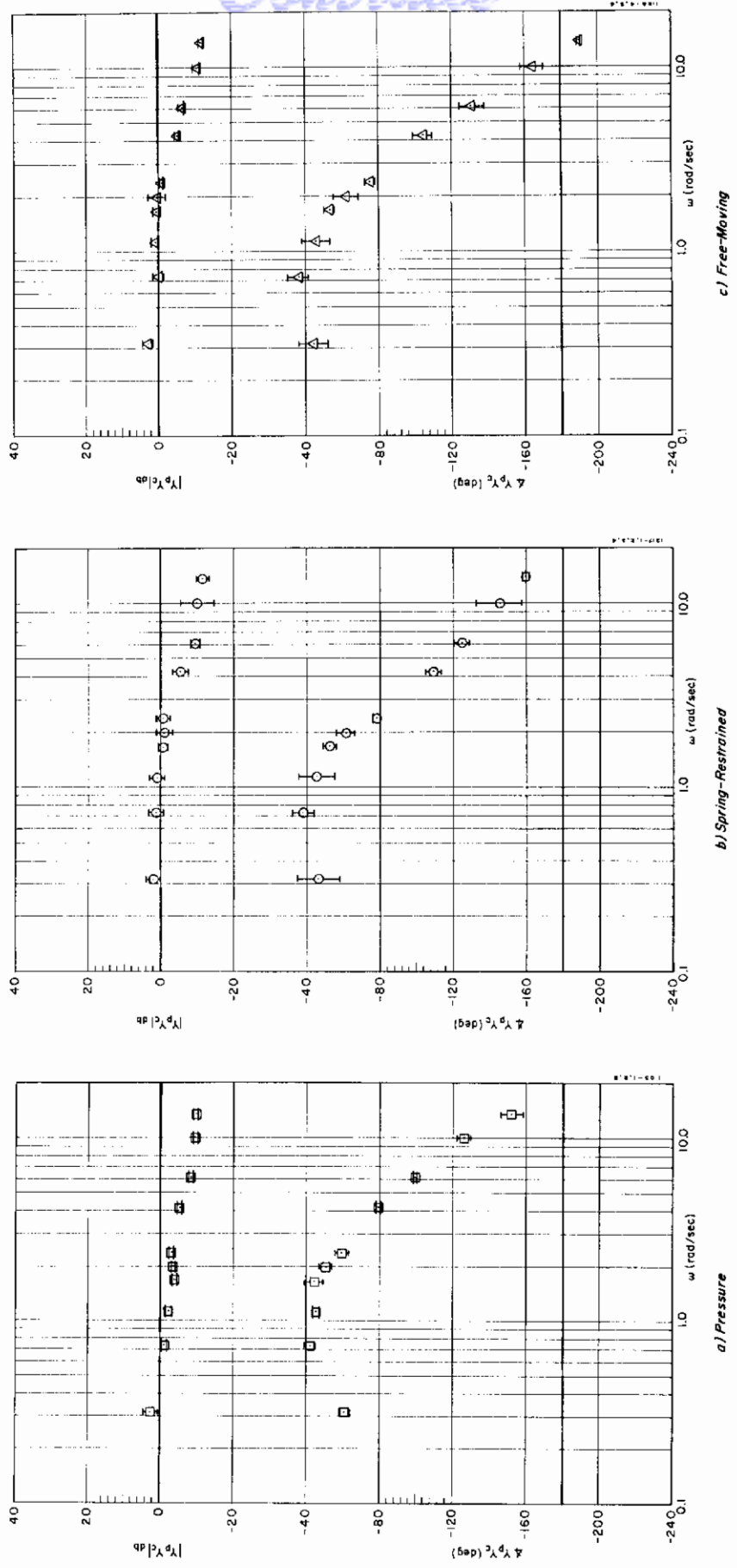


Figure 10. Averaged Describing Functions for Pressure, Spring-Restrained and Free-Moving Manipulators ($R_{2.2}$ Input and $Y_C = 1$)

Contrails

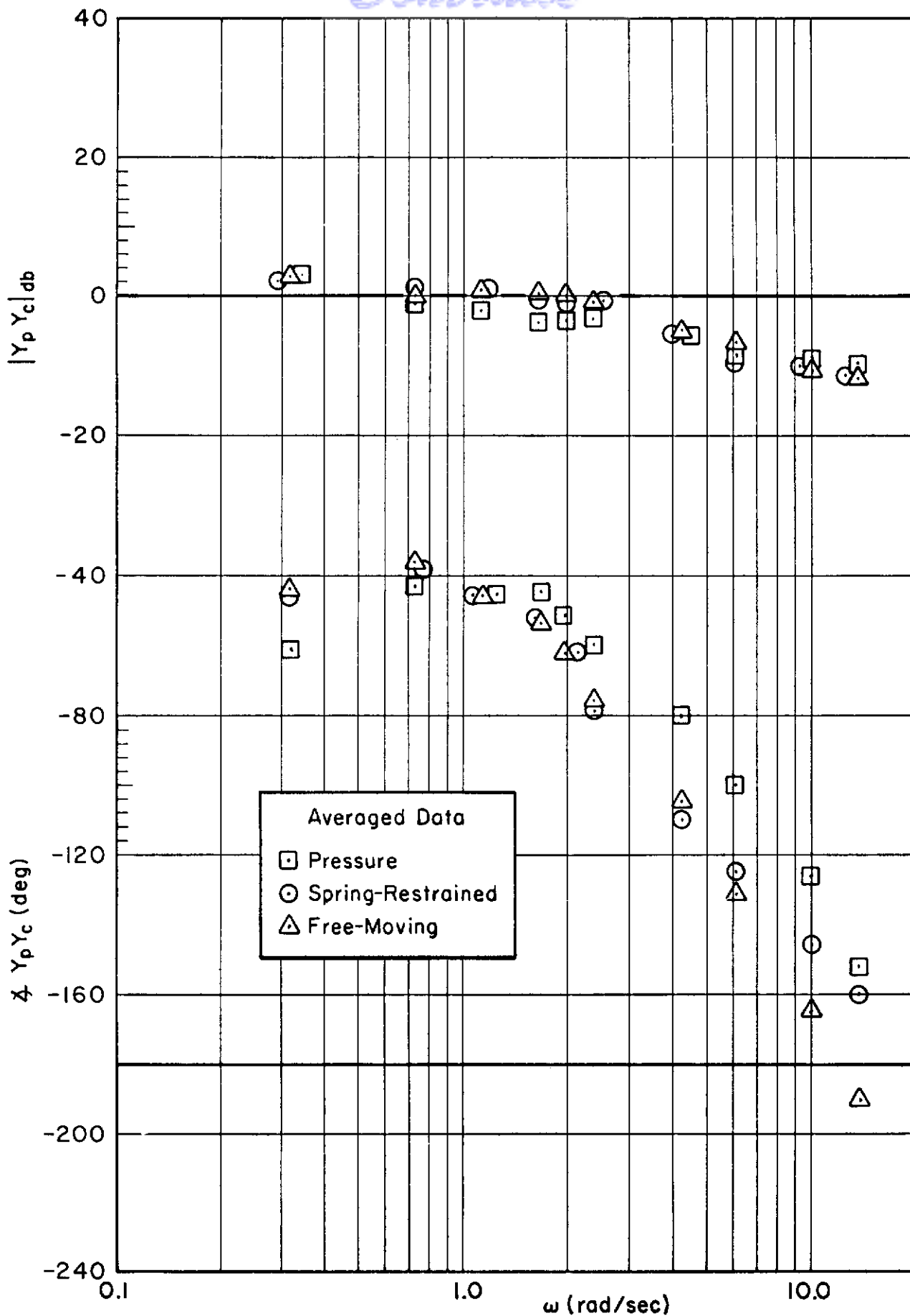


Figure 11. Effects of Manipulators (R2.2 Input and $Y_c = 1$)

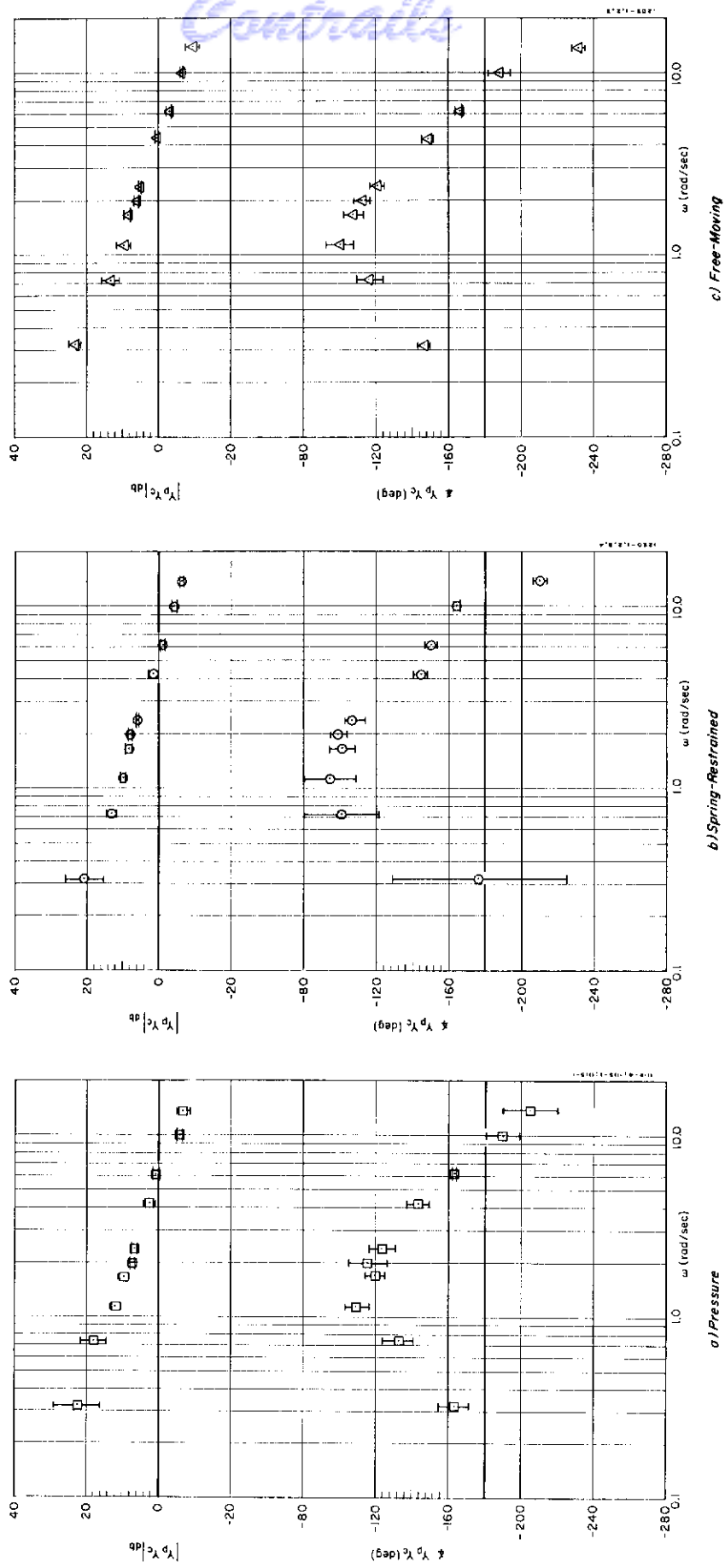


Figure 12. Averaged Describing Functions for Pressure, Spring-Restrained and Free-Moving Manipulators (B_5 Input and $Y_c = 10/s$)

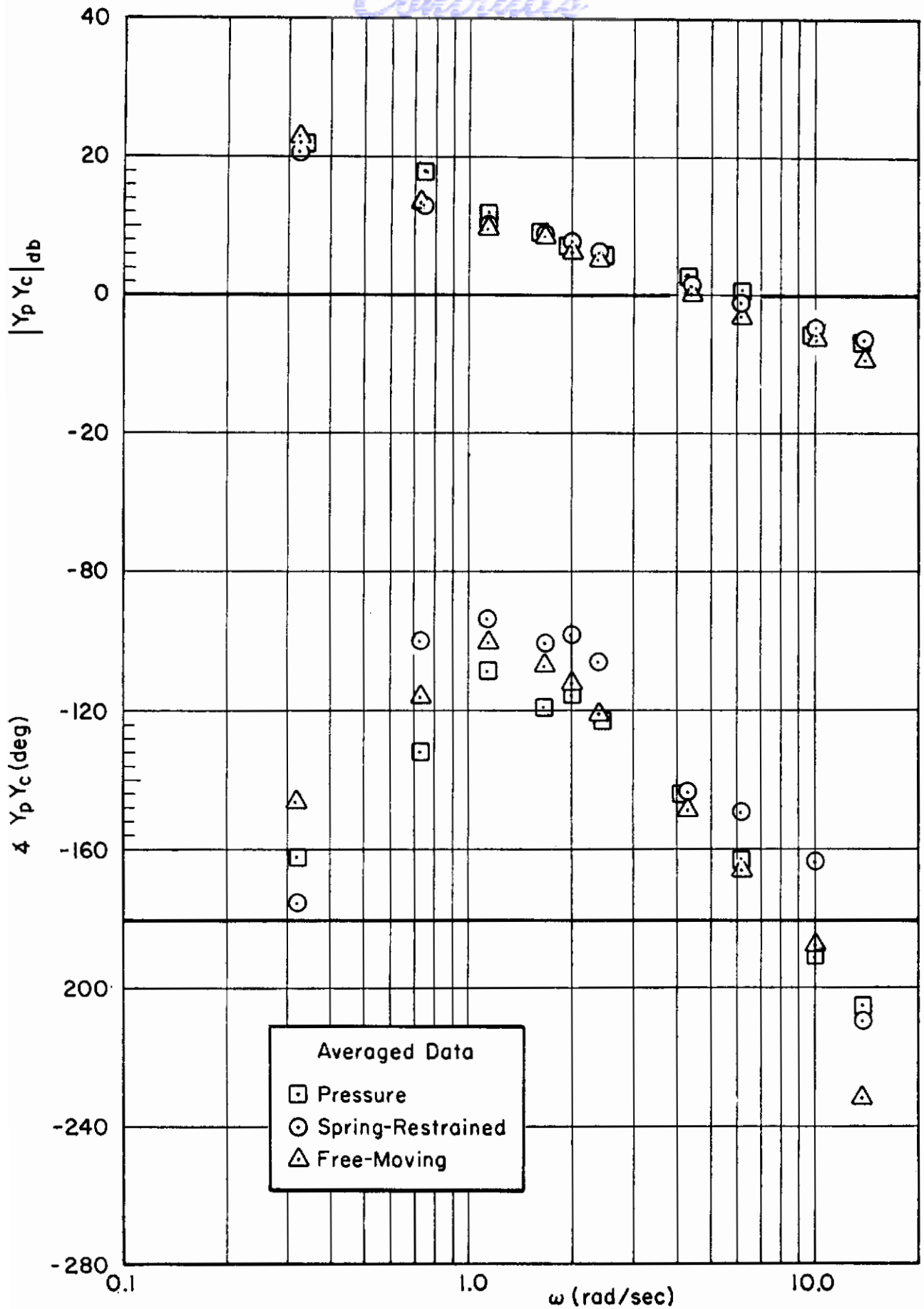


Figure 13. Effects of Manipulators (B5 Input and $Y_c = 10/s$)

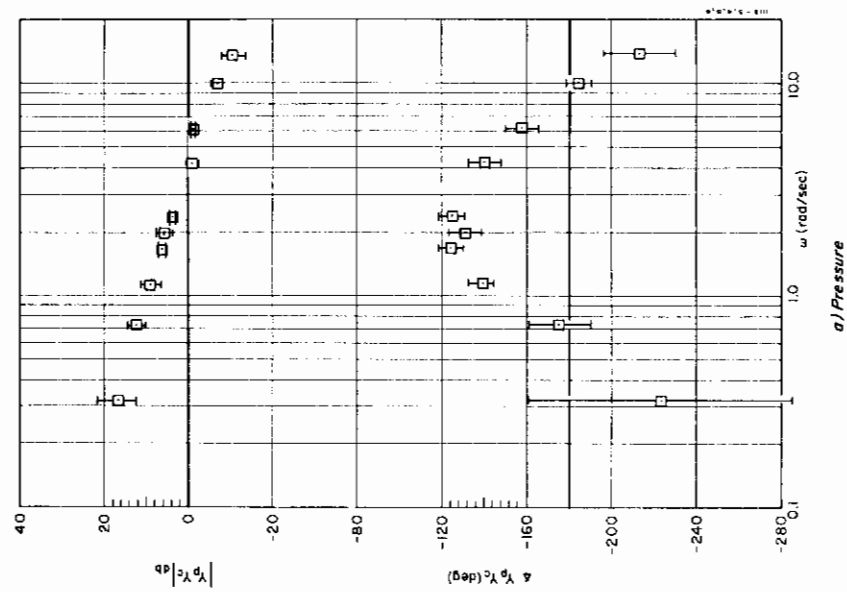
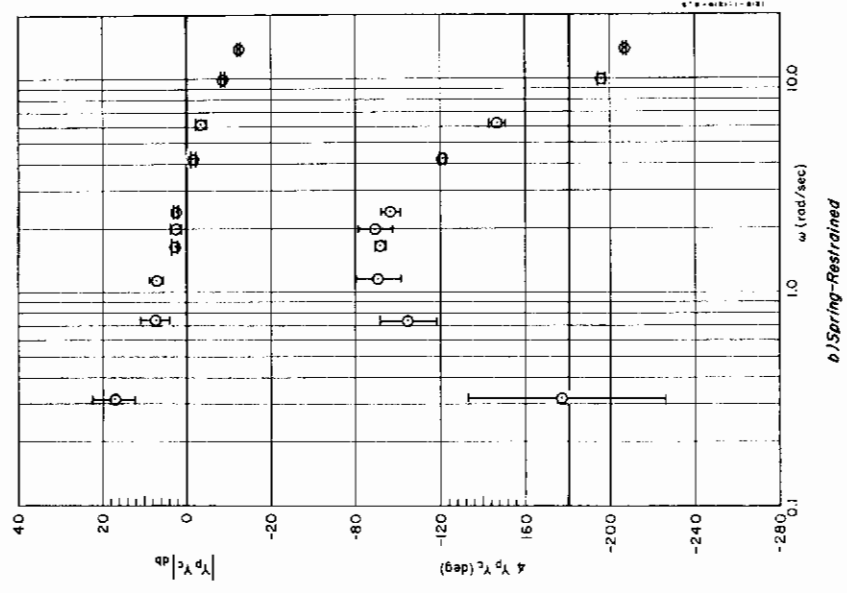
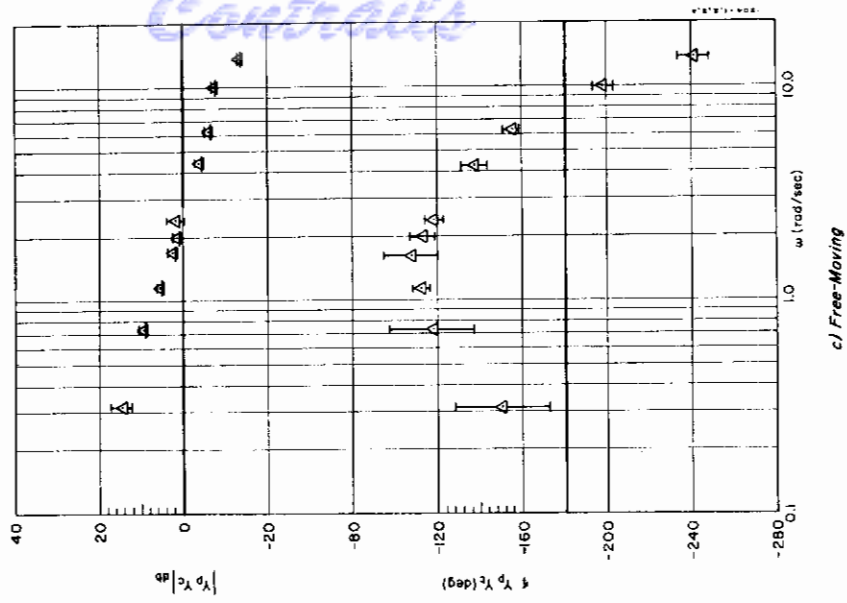


Figure 14. Averaged Describing Functions for Pressure, Spring-Restrained and Free-Moving Manipulators (R2.2 Input and $Y_c = 10/s$)

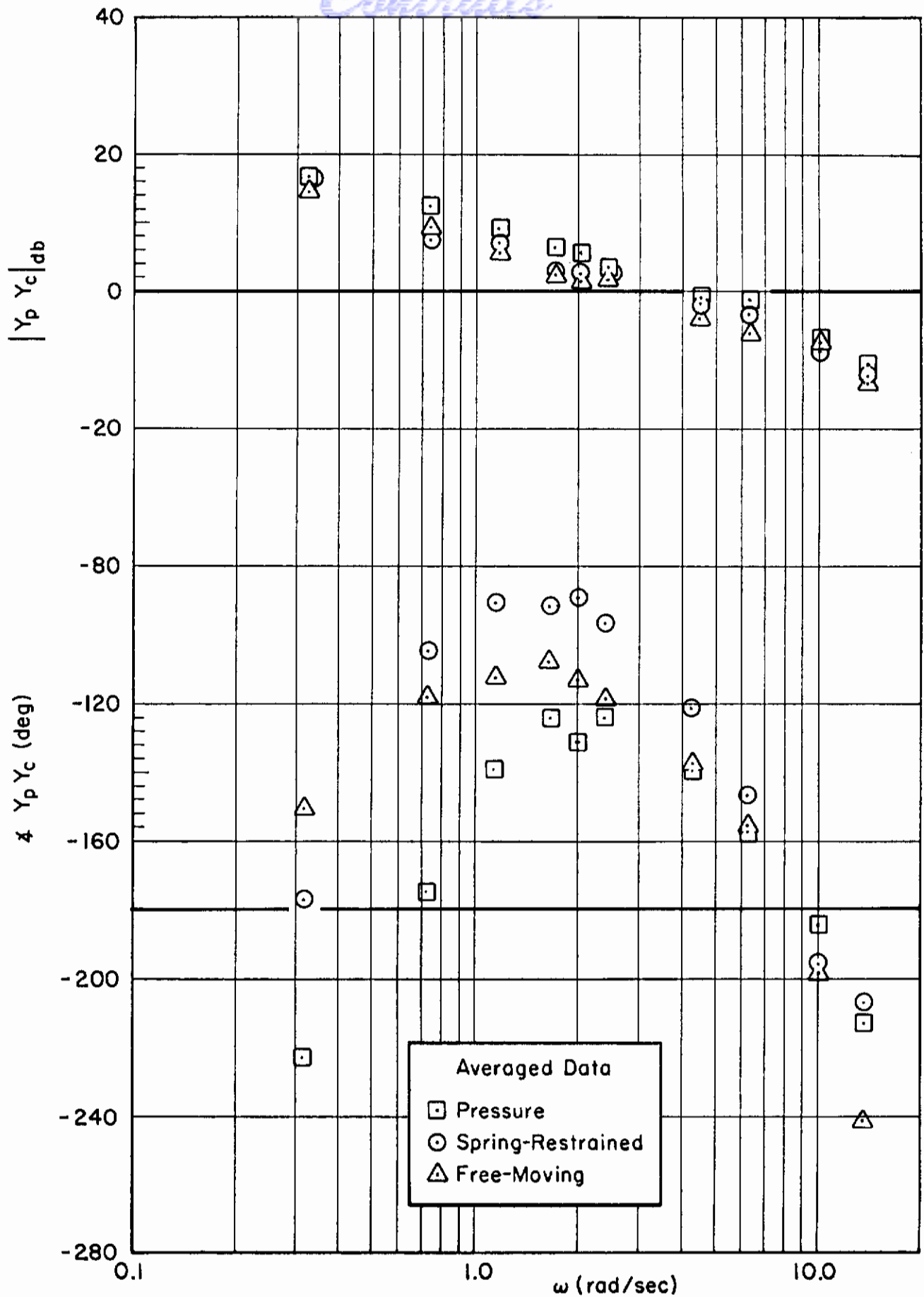


Figure 15. Effects of Manipulators (R2.2 Input and $Y_c = 10/s$)

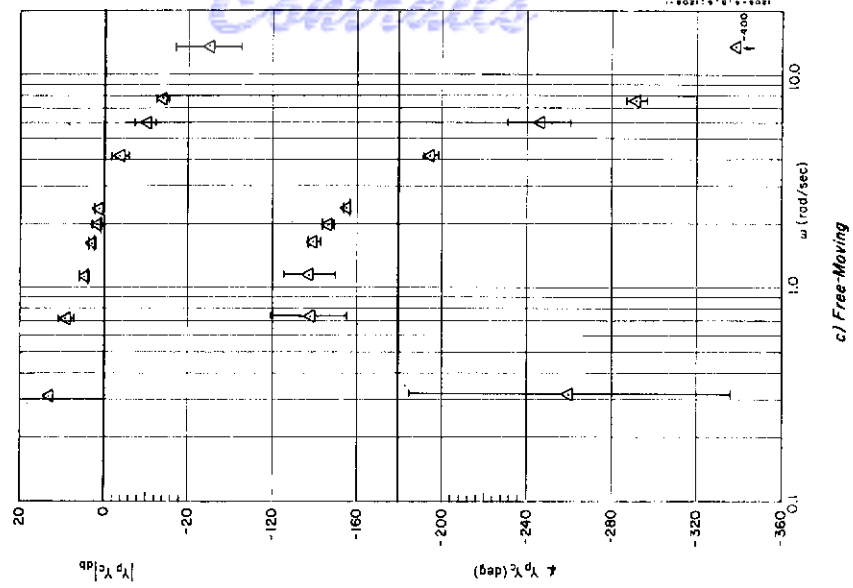
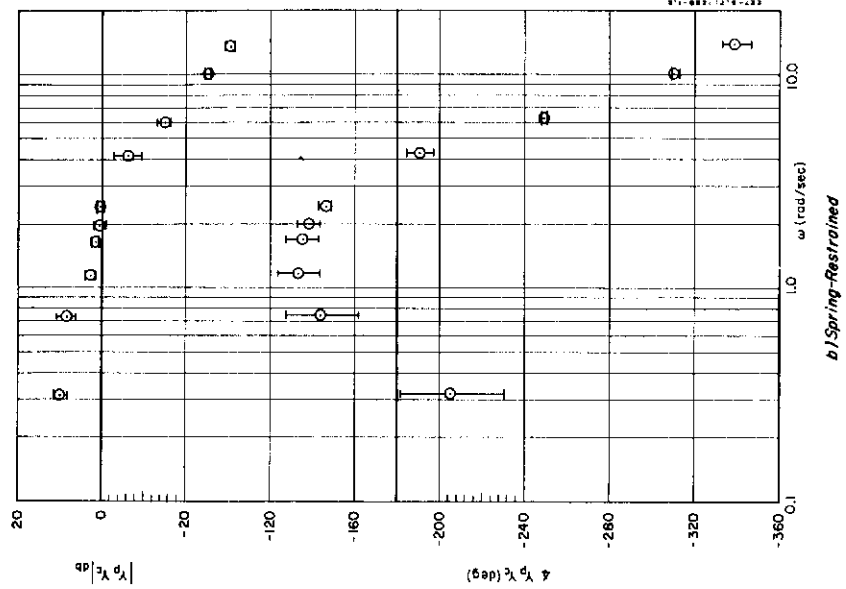
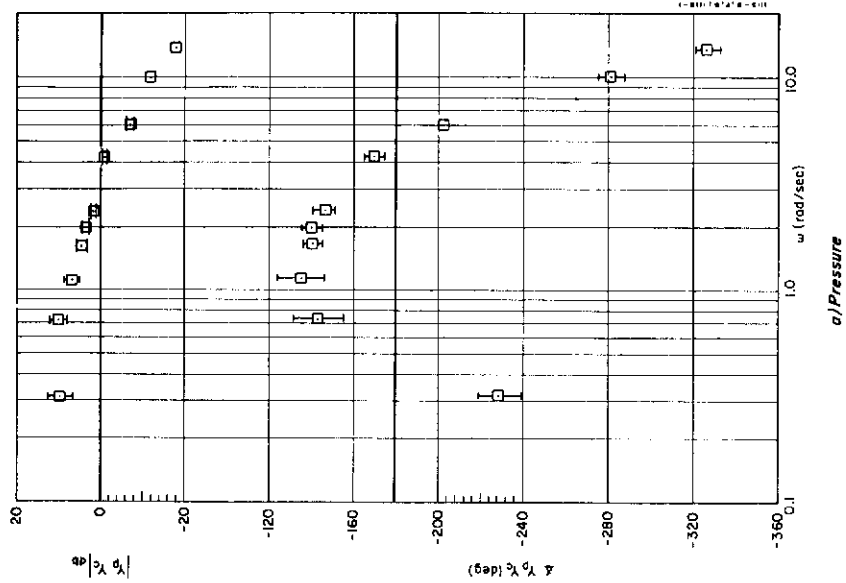


Figure 16. Averaged Describing Functions for Pressure, Spring-Restrained and Free-Moving Manipulators (B5 Input and $Y_C = 5/s^2$)

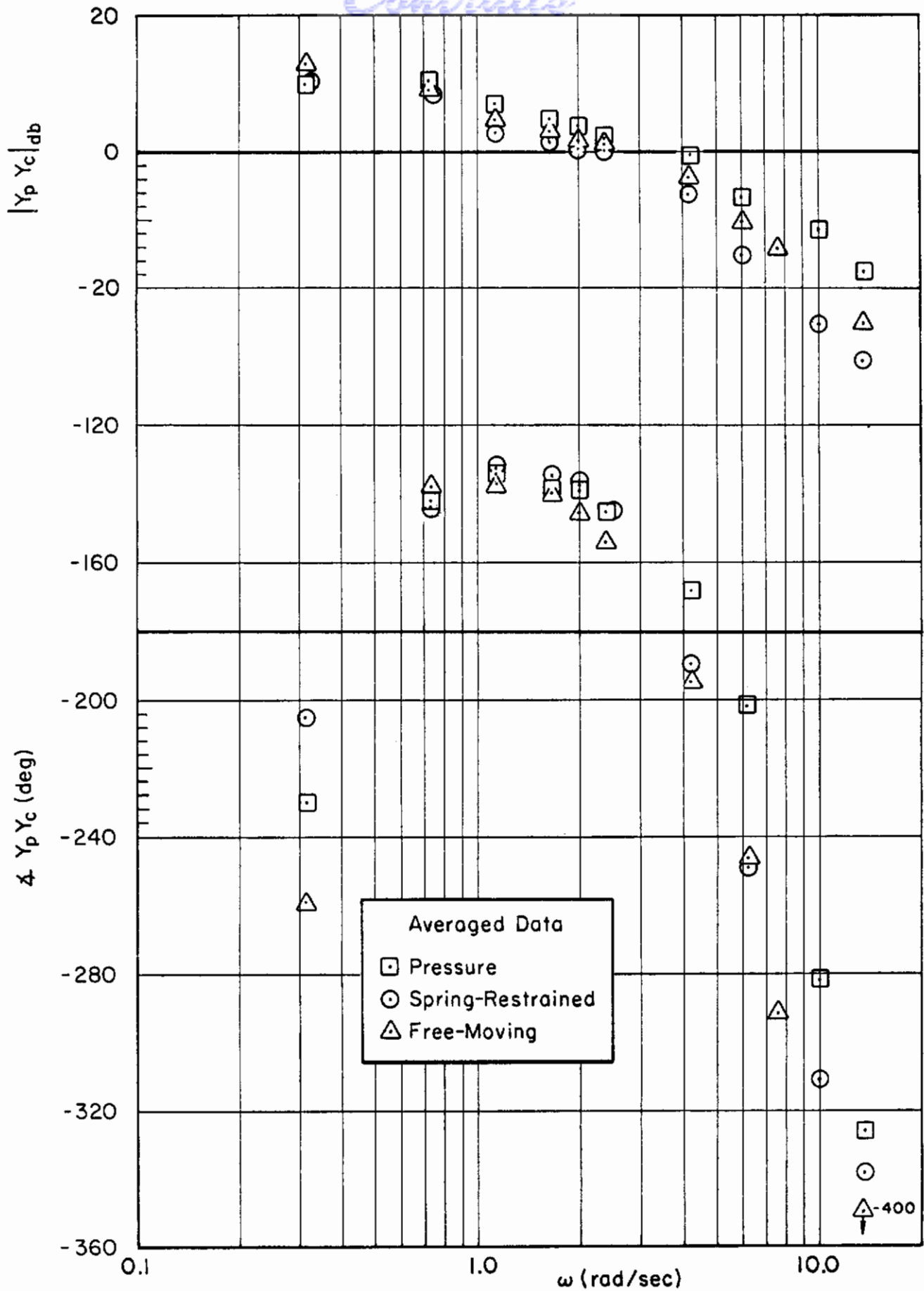


Figure 17. Effects of Manipulators (B5 Input and $Y_c = 5/s^2$)

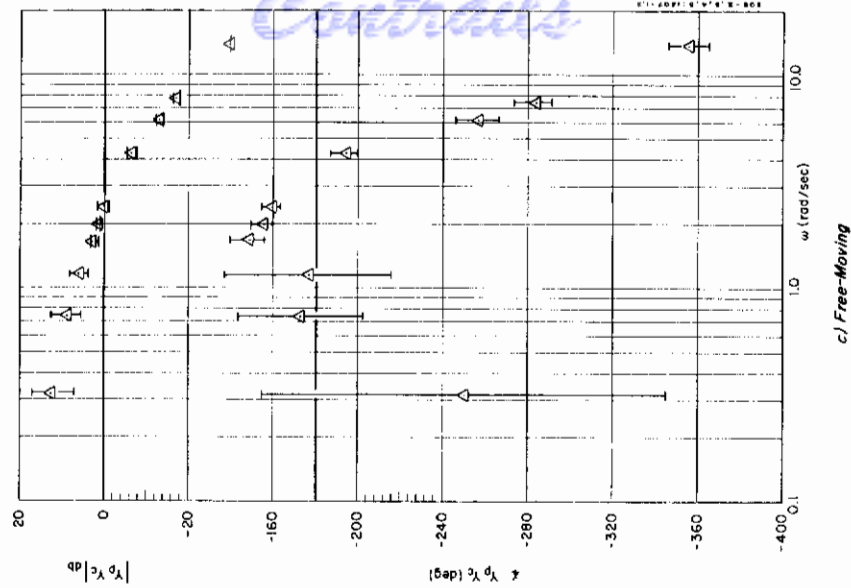
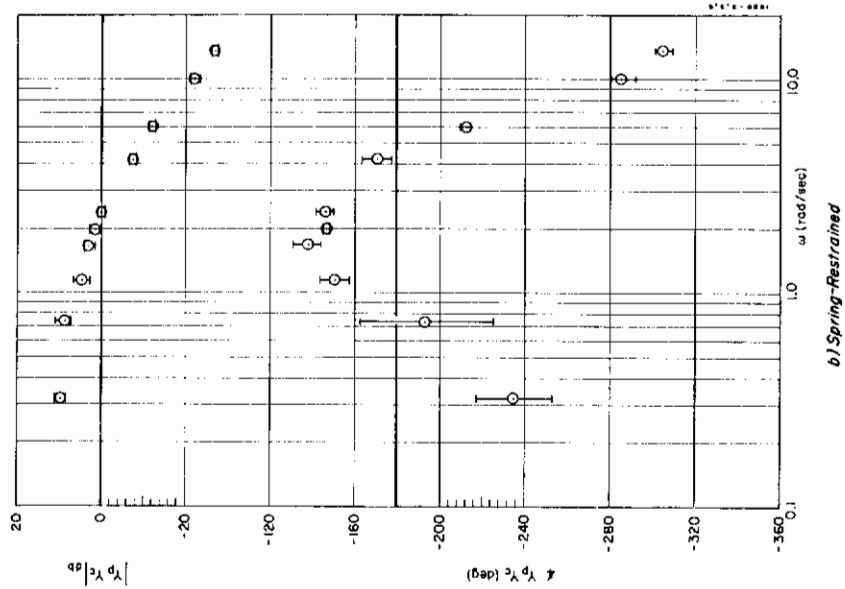
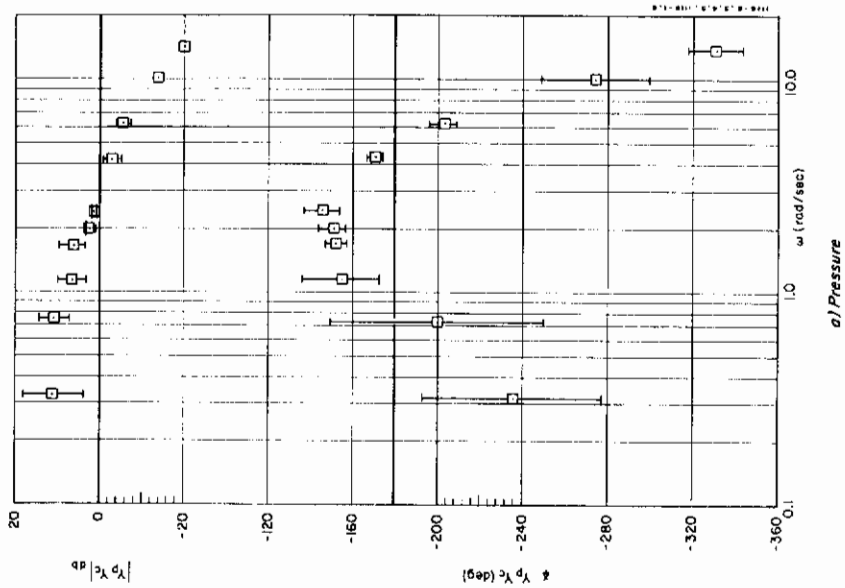


Figure 18. Averaged Describing Functions for Pressure, Spring-Restrained and Free-Moving Manipulators (R2.2 Input and $5/s^2$)

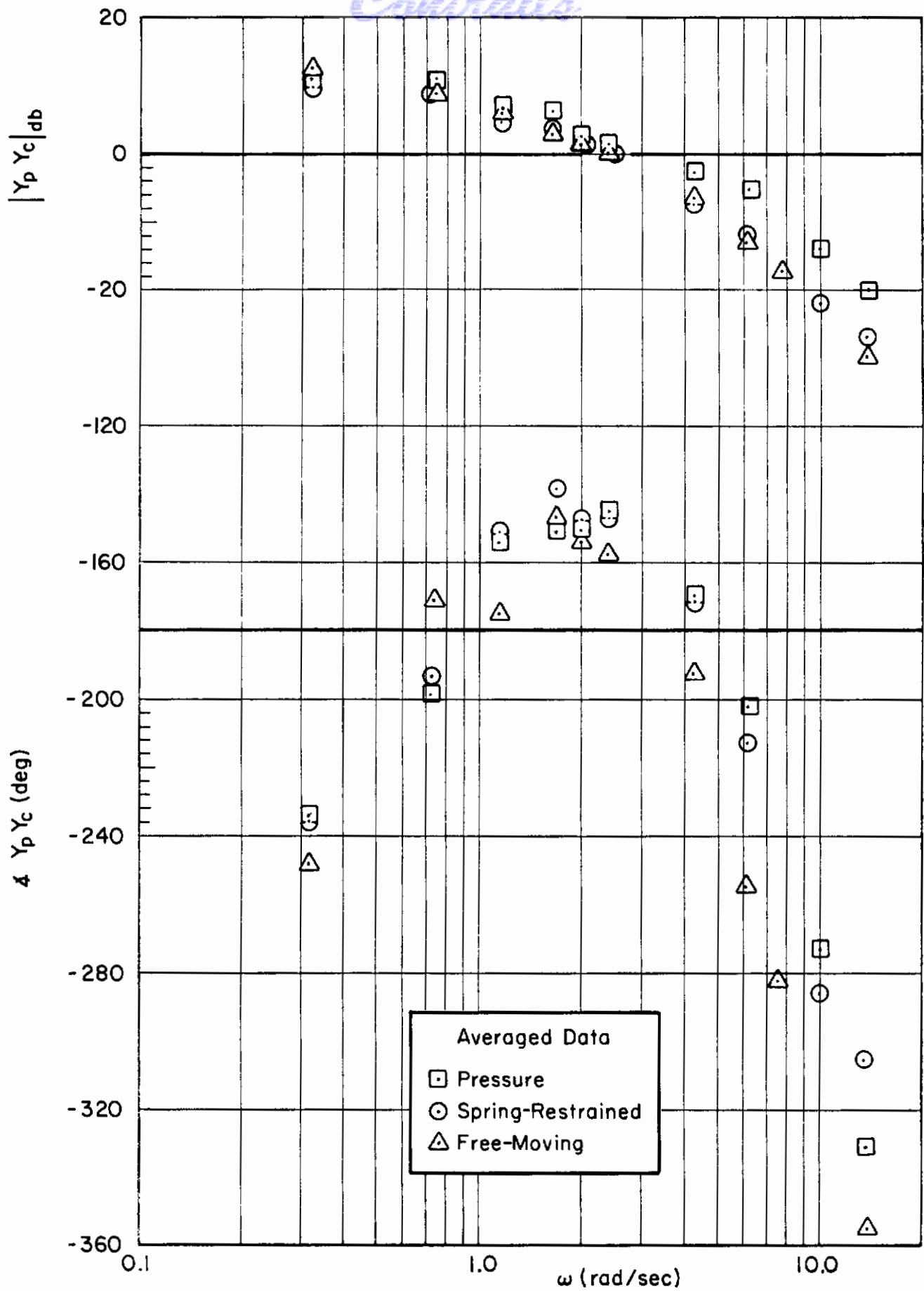
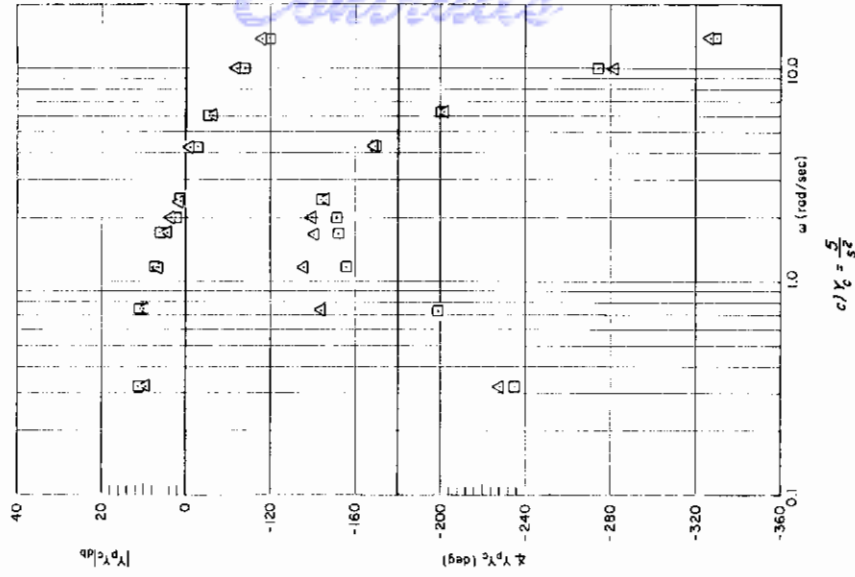
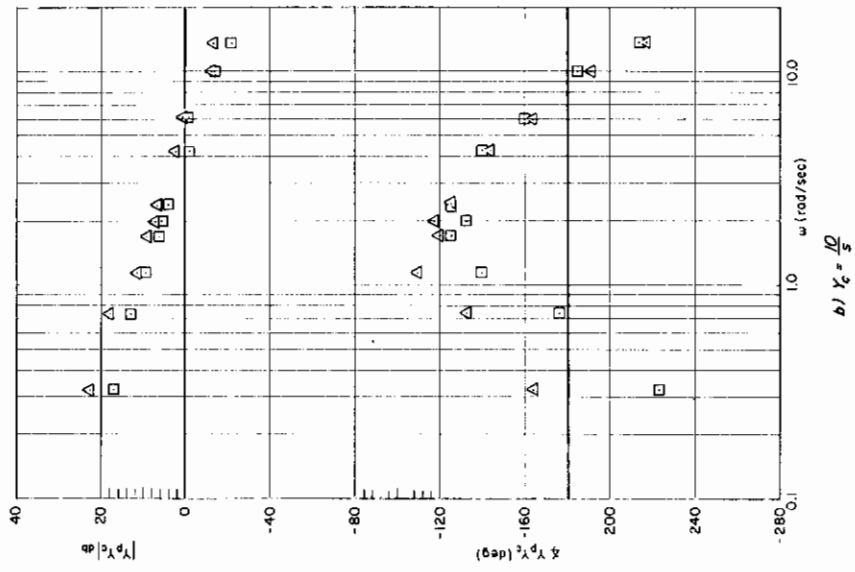
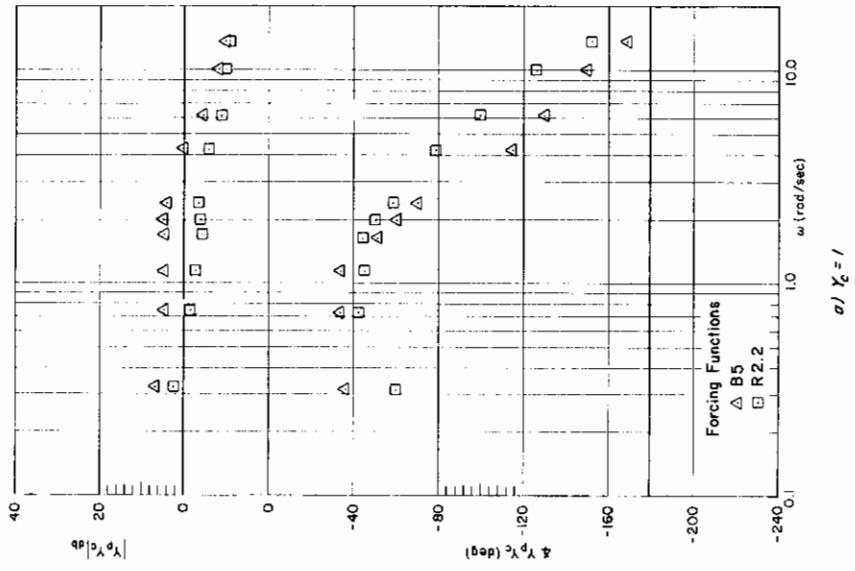


Figure 19. Effects of Manipulators (R2.2 Input and $Y_c = 5/s^2$)



Control

Figure 20. Effects of Forcing Function Bandwidth (Pressure Manipulator)

Controls

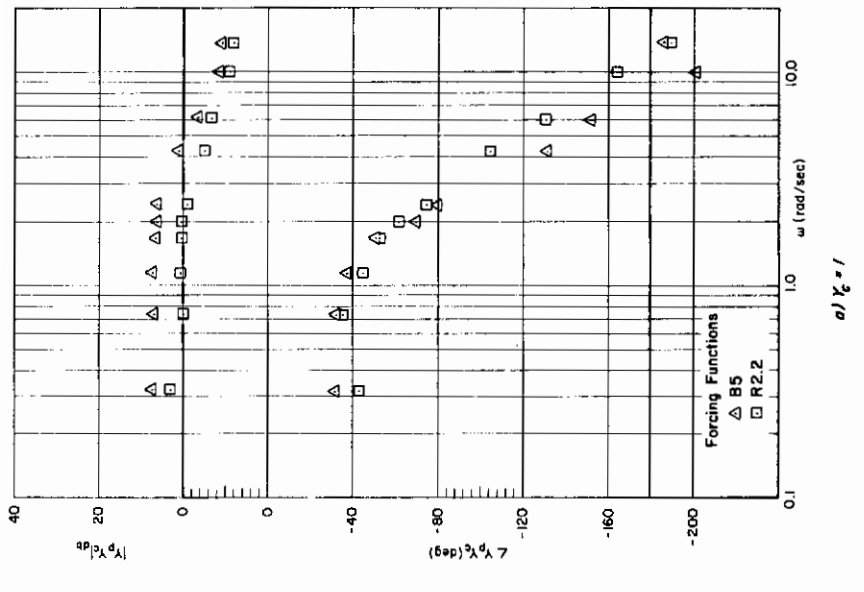
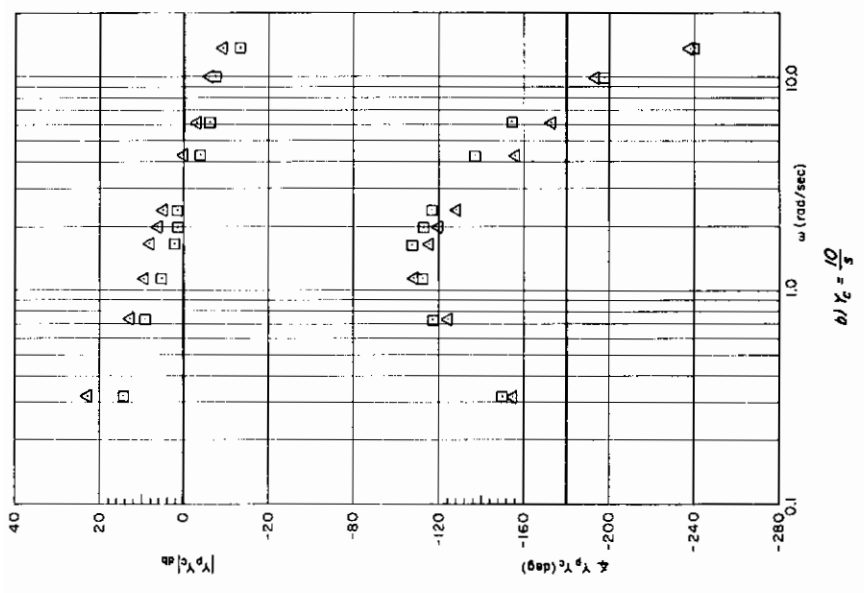
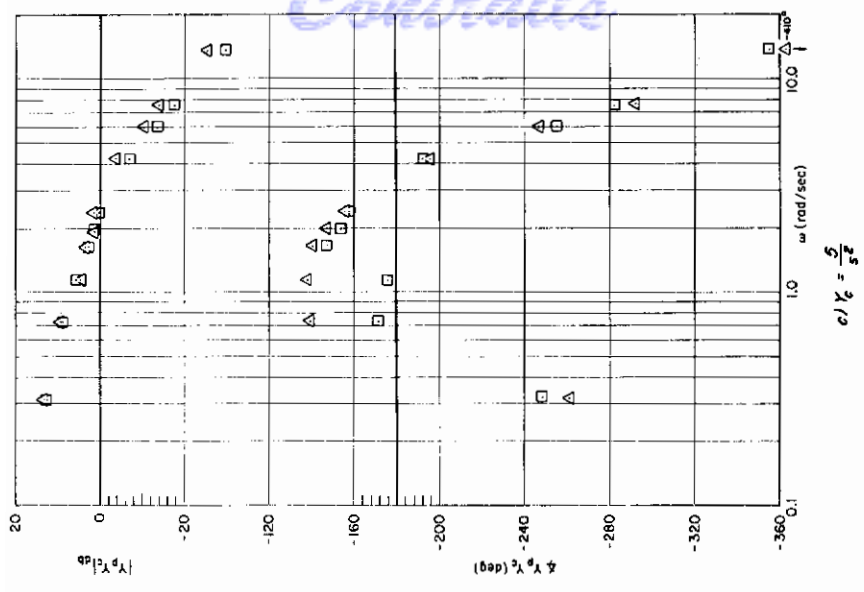


Figure 21. Effects of Forcing Function Bandwidth (Free-Moving)

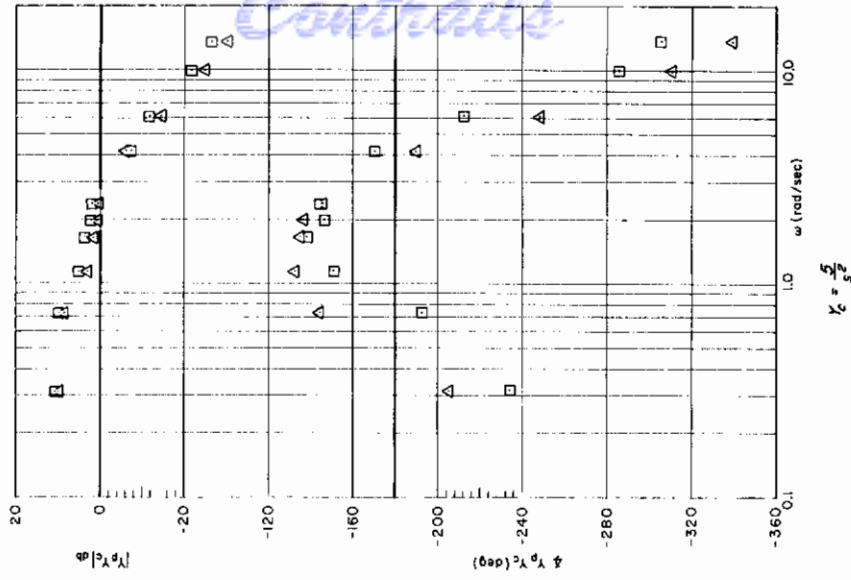
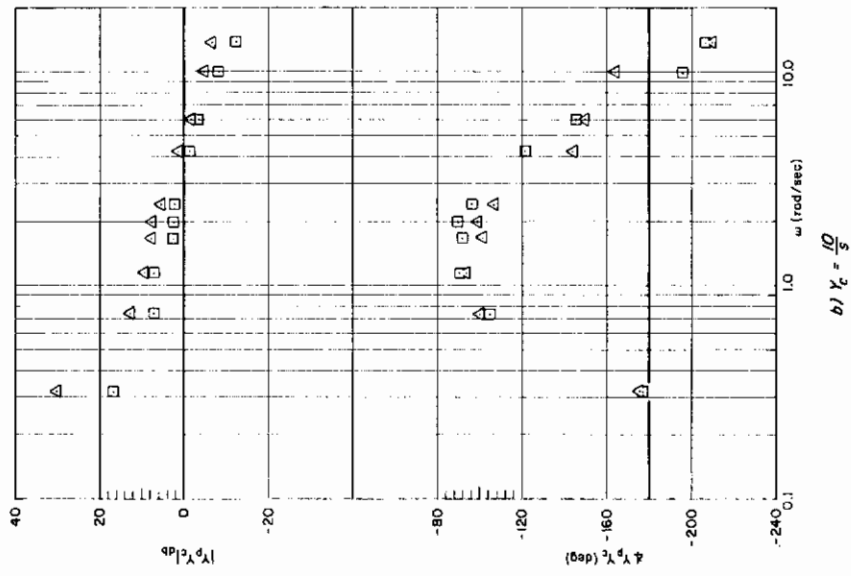
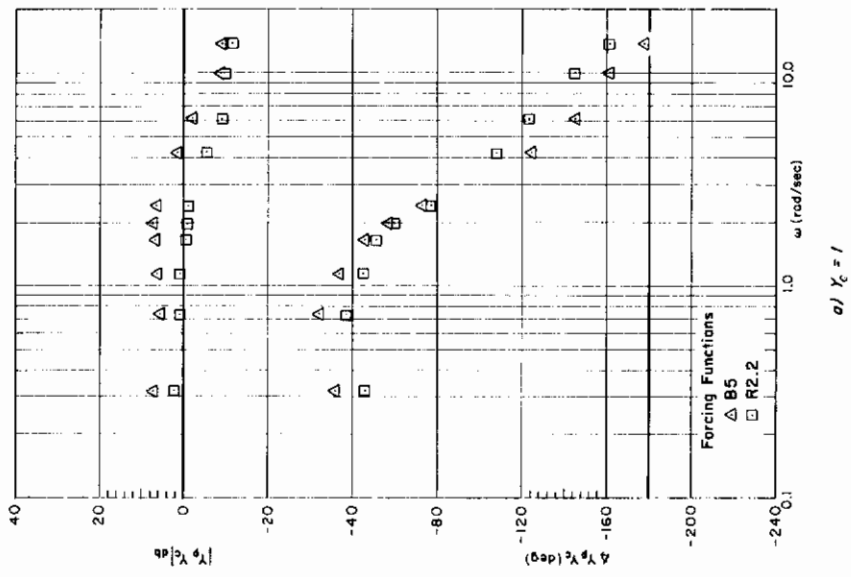


Figure 22. Effects of Forcing Function Bandwidth (Spring-Restrained)

TABLE III

AMPLITUDE RATIO AND PHASE LAG COMPARISONS FOR
FORCING FUNCTION VARIATIONS

CONTROLLED ELEMENT	MANIPULATOR	AMPLITUDE RATIO			PHASE LAG		
		LOW	MID	HIGH	LOW	MID	HIGH
K_c	Pressure	R2.2 Regressive					
	Free-Moving	R2.2 Regressive					
$\frac{K_c}{s}$	Pressure						
	Free-Moving	R2.2 Regressive					
$\frac{K_c}{s^2}$	Pressure						
	Free-Moving						

$B5 \doteq R2.2$

$B5 > R2.2$

$R2.2 > B5$

CHAPTER IV

CONCLUSIONS

The data presented in this report support several conclusions about details which are cited in the discussions of the individual data. In addition, some general conclusions about pressure and free-moving controllers can be drawn from the data as a whole. These include:

1. Almost invariably the RMS error for pressure control is smaller than that for the free-moving control. This result is consonant with that obtained by Gibbs, Ref. 13.
2. For all controlled elements the high frequency phase lag with the free-moving manipulator is greater than that with the pressure manipulator. These data taken in context with the high frequency amplitude ratio data imply that the effective time delay used to represent neuromuscular system lags is less for the pressure than for the free-moving control ($\tau_P < \tau_F$).
3. The low frequency amplitude ratio and phase lag are about the same for both manipulators for $Y_C = K_C/s^2$ and $Y_C = K_C$ (B5 forcing function), implying that $\alpha_P \doteq \alpha_F$ for these controlled elements. For the remaining conditions, i.e., $Y_C = K_C$ (R2.2 forcing function) and $Y_C = K_C/s$, the low frequency phase lag is larger for the pressure control, implying that $\alpha_P > \alpha_F$ for these conditions. Consequently, as a general conclusion $\alpha_P \geq \alpha_F$.
4. In general, changing from a control situation with the free-moving manipulator to one with the pressure control will shift the right side of the phase umbrella toward high frequencies. The left or low frequency side is either maintained at the same level or also shifts toward higher frequencies.

REFERENCES

1. Ashkenas, I. L., and D. T. McRuer, The Determination of Lateral Handling Quality Requirements from Airframe/Human-Pilot System Studies, WADC-TR-59-135, June 1959.
2. Ashkenas, I. L., and D. T. McRuer, "A Theory of Handling Qualities Derived from Pilot-Vehicle System Considerations," Aerospace Eng., Vol. 21, No. 2, Feb. 1962, pp. 60, 61, 83-102.
3. Ashkenas, I. L., and T. S. Durand, "Simulator and Analytical Studies of Fundamental Longitudinal Control Problems in Carrier Approach," AIAA Simulation for Aerospace Flight Conference, A Volume of Technical Papers Presented Aug. 26-28, 1963, Columbus, Ohio, AIAA, New York, 1963, pp. 16-34.
4. Ashkenas, I. L., H. R. Jex, and D. T. McRuer, Pilot-Induced Oscillations: Their Cause and Analysis, Northrop Corporation, Norair Division, Rept. NOR 64-143 (Systems Technology, Inc., TR-239-2), 20 June 1964.
5. Bower, John L., and Peter M. Schultheiss, Introduction to the Design of Servomechanisms, John Wiley and Sons, New York, 1958.
6. Cromwell, C. H., and I. L. Ashkenas, A Systems Analysis of Longitudinal Piloted Control in Carrier Approach, Systems Technology, Inc., TR-124-1, June 1962.
7. Durand, T. S., and H. R. Jex, Handling Qualities in Single-Loop Roll Tracking Tasks: Theory and Simulator Experiments, ASD-TDR-62-507, Nov. 1962.
8. Durand, T. S., and G. L. Teper, An Analysis of Terminal Flight Path Control in Carrier Landings, Systems Technology, Inc., TR-137-1, Aug. 1964.
9. Elkind, J. I., Characteristics of Simple Manual Control Systems, MIT, Lincoln Laboratory, TR-111, 6 Apr. 1956.
10. Elkind, J. I., "A Survey of the Development of Models for the Human Controller," Guidance and Control—II, ed. R. C. Langford and C. J. Mundo (Progress in Astronautics and Aeronautics, Vol. 13) Academic Press, New York, June 1964, pp. 623-643.
11. Elkind, J. I., and D. L. Darley, "The Normality of Signals and Describing Function Measurements of Simple Manual Control Systems," IEEE Trans., Vol. HFE-4, No. 1, Sept. 1963, pp. 52-55.
12. Frost, G. G., An Application of a Dynamic Pilot-Model to System Design, ASD-TN-61-57, Apr. 1961.

Contrails

13. Gibbs, C. B., "The Continuous Regulation of Skilled Response by Kinaesthetic Feedback," The British Journal of Psychology (General Section), Vol. XLV, Part 1, Feb. 1954, pp. 24-39.
14. Investigation of Control "Feel" Effects on the Dynamics of a Piloted Aircraft System, Goodyear Aircraft Corporation Rept. GER-6726, Apr. 25, 1955.
15. Graham, D., and D. McRuer, Analysis of Nonlinear Control Systems, John Wiley and Sons, New York, 1961.
16. Hall, I. A. M., Effects of Controlled Element on the Human Pilot, WADC-TR-57-509, Aug. 1958.
17. Hall, I. A. M., "Study of the Human Pilot as a Servo-Element," J. Royal Aeron. Society, Vol. 67, No. 630, June 1963, pp. 351-360.
18. Jex, H. R., and C. H. Cromwell, Theoretical and Experimental Investigation of Some New Longitudinal Handling Quality Parameters, ASD-TR-61-26, Mar. 1961.
19. Krendel, E. S., and D. T. McRuer, "A Servomechanisms Approach to Skill Development," J. Franklin Inst., Vol. 269, No. 1, Jan. 1960, pp. 24-42.
20. Krendel, E. S., and G. H. Barnes, Interim Report on Human Frequency Response Studies, WADC-TR-54-370, June 1954.
21. Licklider, J. C. R., "Quasi-Linear Operator Models in the Study of Manual Tracking," Developments in Mathematical Psychology, ed. R. Duncan Luce, The Free Press of Glencoe, Ill., 1960, pp. 169-279.
22. Loller, T. E., and J. Matous, "Observed Pilot-Vehicle Loop-Closure Characteristics for Hovering Aircraft Control," IEEE Trans., Vol. HFE-4, No. 1, Sept. 1963, pp. 60-63.
23. McRuer, D. T., and E. S. Krendel, Dynamic Response of Human Operators, WADC-TR-56-524, Oct. 1957.
24. McRuer, D. T., and E. S. Krendel, "The Human Operator as a Servo System Element," J. Franklin Inst., Vol. 267, No. 5, May 1959, pp. 381-403; No. 6, June 1959, pp. 511-536.
25. McRuer, D. T., I. L. Ashkenas, and C. L. Guerre, A Systems Analysis View of Longitudinal Flying Qualities, WADD-TR-60-43, Jan. 1960.
26. McRuer, D. T., and R. E. Magdaleno, Human Pilot Dynamic Response in Single-Loop System with Compensatory and Pursuit Displays, AFFDL-TR-66-137, Dec. 1966.

Contrails

27. McRuer, Duane, Dunstan Graham, Ezra Krendel, and William Reisener, Jr., Human Pilot Dynamics in Compensatory Systems: Theory, Models, and Experiments with Controlled Element and Forcing Function Variations, AFFDL-TR-65-15, July 1965.
28. McRuer, D. T., Some Statistical Properties of Time Functions Composed of Sinusoids, Systems Technology, Inc., TM-80, 9 Mar. 1961.
29. Magdaleno, R. E., WHM Analyzer Finite Run Length Errors, Systems Technology, Inc., TM-84, 8 Mar. 1961.
30. McRuer, D. T., and R. E. Magdaleno, Effects of Manipulator Restraints on Human Operator Performance, AFFDL-TR-66-72, Dec. 1966.
31. Muckler, F. A., and R. W. Obermayer, The Use of Man in Booster Guidance and Control, AIAA Paper 63-312, Aug. 1963. (Also published as NASA CR-81, July 1964.)
32. Russell, Lindsay, Characteristics of the Human as a Linear Servo-Element, Master's thesis, MIT, Dept. of Electrical Eng., May 18, 1951.
33. Sadoff, M., The Effects of Longitudinal Control-System Dynamics on Pilot Opinion and Response Characteristics as Determined from Flight Tests and from Ground Simulator Studies, NASA Memo 10-1-58A, Oct. 1958.
34. Seckel, E., I. A. M. Hall, D. T. McRuer, and D. H. Weir, Human Pilot Dynamic Response in Flight and Simulator, WADC-TR-57-520, Oct. 1957.
35. Sheridan, T. B., "The Human Operator in Control Instrumentation," Progress in Control Engineering, Vol. I, ed. R. H. Macmillan, T. J. Higgins, and P. Naslin, Academic Press, New York, 1962, pp. 141-187.
36. Slack, M., "The Probability Distribution of Sinusoidal Oscillations Combined in Random Noise," Jour. IEE (London), Vol. 93, Pt. III, 1945.
37. Smith, R. H., "On the Limits of Manual Control," IEEE Trans., Vol. HFE-4, No. 1, Sept. 1963, pp. 56-59.
38. Stapleford, R. L., D. E. Johnston, G. L. Teper, and D. H. Weir, A Method for Evaluating the Lateral-Directional Handling Qualities of a Supersonic Transport in the Landing Approach and Assessing Competing Augmentation Systems, Systems Technology, Inc., Tech. Rept. 131-1, Dec. 1963.
39. Taylor, L. W., Jr., Analysis of a Pilot-Airplane Lateral Instability Experienced with the X-15 Airplane, NASA TN D-1059, Nov. 1961.

Contrails

40. Teper, Gary L., and Robert L. Stapleford, "An Assessment of the Lateral-Directional Handling Qualities of a Large Aircraft in the Landing Approach," J. Aircraft, Vol. 3, No. 3, May-June 1966.
41. Tustin, A., "The Nature of the Operator's Response in Manual Control and Its Implications for Controller Design," J. IEEE, Vol. 94, Part IIA, No. 2, 1947.

Unclassified

Security Classification

DOCUMENT CONTROL DATA - R&D		
<i>(Security classification of title, body of abstract and indexing annotation must be entered when the overall report is classified)</i>		
1. ORIGINATING ACTIVITY (Corporate author) Systems Technology, Incorporated 13766 South Hawthorne Boulevard Hawthorne, California 90250		2a. REPORT SECURITY CLASSIFICATION Unclassified
		2b. GROUP N/A
3. REPORT TITLE Human Pilot Dynamics With Various Manipulators		
4. DESCRIPTIVE NOTES (Type of report and inclusive dates) Final Technical Report		
5. AUTHOR(S) (Last name, first name, initial) McRuer, D. T. Magdaleno, R. E.		
6. REPORT DATE December 1966	7a. TOTAL NO. OF PAGES 42	7b. NO. OF REFS 41
8a. CONTRACT OR GRANT NO. AF 33(657)-10835	9a. ORIGINATOR'S REPORT NUMBER(S) AFFIL-TR-66-138	
b. PROJECT NO. 8219		
c. Task: 821905	9b. OTHER REPORT NO(S) (Any other numbers that may be assigned this report) STI-TR-134-3	
d.		
10. AVAILABILITY/LIMITATION NOTICES Distribution of this document is unlimited.		
11. SUPPLEMENTARY NOTES	12. SPONSORING MILITARY ACTIVITY AFFIL (FDCC) Wright-Patterson AFB, Ohio 45433	
13. ABSTRACT The purpose of the experimental efforts reported here is to explore on a preliminary basis the limiting characteristics of the human operator's "actuator" or neuromuscular system dynamics as affected by the manipulator. The effects of three manipulators (pressure, free-moving, and spring-restrained) on system performance and the human operator's describing function are presented for three controlled elements and two high bandwidth forcing functions.		

DD FORM 1473
1 JAN 64

Unclassified

Security Classification

14. KEY WORDS Human Response Manipulators Human Engineering Flight Control Systems Pilot Models	LINK A		LINK B		LINK C	
	ROLE	WT	ROLE	WT	ROLE	WT

INSTRUCTIONS

1. **ORIGINATING ACTIVITY:** Enter the name and address of the contractor, subcontractor, grantee, Department of Defense activity or other organization (*corporate author*) issuing the report.

2a. **REPORT SECURITY CLASSIFICATION:** Enter the overall security classification of the report. Indicate whether "Restricted Data" is included. Marking is to be in accordance with appropriate security regulations.

2b. **GROUP:** Automatic downgrading is specified in DoD Directive 5200.10 and Armed Forces Industrial Manual. Enter the group number. Also, when applicable, show that optional markings have been used for Group 3 and Group 4 as authorized.

3. **REPORT TITLE:** Enter the complete report title in all capital letters. Titles in all cases should be unclassified. If a meaningful title cannot be selected without classification, show title classification in all capitals in parenthesis immediately following the title.

4. **DESCRIPTIVE NOTES:** If appropriate, enter the type of report, e.g., interim, progress, summary, annual, or final. Give the inclusive dates when a specific reporting period is covered.

5. **AUTHOR(S):** Enter the name(s) of author(s) as shown on or in the report. Enter last name, first name, middle initial. If military, show rank and branch of service. The name of the principal author is an absolute minimum requirement.

6. **REPORT DATE:** Enter the date of the report as day, month, year; or month, year. If more than one date appears on the report, use date of publication.

7a. **TOTAL NUMBER OF PAGES:** The total page count should follow normal pagination procedures, i.e., enter the number of pages containing information.

7b. **NUMBER OF REFERENCES:** Enter the total number of references cited in the report.

8a. **CONTRACT OR GRANT NUMBER:** If appropriate, enter the applicable number of the contract or grant under which the report was written.

8b, 8c, & 8d. **PROJECT NUMBER:** Enter the appropriate military department identification, such as project number, subproject number, system numbers, task number, etc.

9a. **ORIGINATOR'S REPORT NUMBER(S):** Enter the official report number by which the document will be identified and controlled by the originating activity. This number must be unique to this report.

9b. **OTHER REPORT NUMBER(S):** If the report has been assigned any other report numbers (*either by the originator or by the sponsor*), also enter this number(s).

10. **AVAILABILITY/LIMITATION NOTICES:** Enter any limitations on further dissemination of the report, other than those

imposed by security classification, using standard statements such as:

- (1) "Qualified requesters may obtain copies of this report from DDC."
- (2) "Foreign announcement and dissemination of this report by DDC is not authorized."
- (3) "U. S. Government agencies may obtain copies of this report directly from DDC. Other qualified DDC users shall request through _____."
- (4) "U. S. military agencies may obtain copies of this report directly from DDC. Other qualified users shall request through _____."
- (5) "All distribution of this report is controlled. Qualified DDC users shall request through _____."

If the report has been furnished to the Office of Technical Services, Department of Commerce, for sale to the public, indicate this fact and enter the price, if known.

11. **SUPPLEMENTARY NOTES:** Use for additional explanatory notes.

12. **SPONSORING MILITARY ACTIVITY:** Enter the name of the departmental project office or laboratory sponsoring (*paying for*) the research and development. Include address.

13. **ABSTRACT:** Enter an abstract giving a brief and factual summary of the document indicative of the report, even though it may also appear elsewhere in the body of the technical report. If additional space is required, a continuation sheet shall be attached.

It is highly desirable that the abstract of classified reports be unclassified. Each paragraph of the abstract shall end with an indication of the military security classification of the information in the paragraph, represented as (TS), (S), (C), or (U).

There is no limitation on the length of the abstract. However, the suggested length is from 150 to 225 words.

14. **KEY WORDS:** Key words are technically meaningful terms or short phrases that characterize a report and may be used as index entries for cataloging the report. Key words must be selected so that no security classification is required. Identifiers, such as equipment model designation, trade name, military project code name, geographic location, may be used as key words but will be followed by an indication of technical context. The assignment of links, rules, and weights is optional.